

---

# Auto-tune: PAC-Bayes Optimization over Prior and Posterior for Neural Networks

---

Xitong Zhang<sup>1</sup>, Avrajit Ghosh<sup>1</sup>, Guangliang Liu<sup>2</sup>, and Rongrong Wang<sup>1,3</sup>

<sup>1</sup>Computational Mathematics Science and Engineering , Michigan State University

<sup>2</sup>Computer Science and Engineering , Michigan State University

<sup>3</sup>Department of Mathematics , Michigan State University

## Abstract

It is widely recognized that the generalization ability of neural networks can be greatly enhanced through carefully designing the training procedure. The current state-of-the-art training approach involves utilizing stochastic gradient descent (SGD) or Adam optimization algorithms along with a combination of additional regularization techniques such as weight decay, dropout, or noise injection. Optimal generalization can only be achieved by tuning a multitude of hyperparameters through grid search, which can be time-consuming and necessitates additional validation datasets. To address this issue, we introduce a practical PAC-Bayes training framework that is nearly tuning-free and requires no additional regularization while achieving comparable testing performance to that of SGD/Adam after a complete grid search and with extra regularizations. Our proposed algorithm demonstrates the remarkable potential of PAC training to achieve state-of-the-art performance on deep neural networks with enhanced robustness and interpretability.

## 1 Introduction

PAC-Bayes generalization bounds serve as a critical theoretical foundation for contemporary deep learning, by providing quantitative assessments of the ability of trained neural network models to effectively generalize to unobserved test data [49], [40], [41]. Although PAC-Bayes bounds were traditionally used only in the post-training stage for the purpose of quality control [52, 41], the recent work of Dziugaite et al.[16] has opened the door to using these bounds during the training phase. They showed that one can directly train a network via optimizing the PAC-Bayes bounds, a strategy we refer to as PAC-Bayes training, and obtained reasonable performances. This discovery marks the first time PAC-Bayes bounds have been leveraged for training a neural network and has sparked further exploration into various other PAC-Bayes training techniques [33], [47], [45], [6],[44],[18],[15]. However, it is well-known that the PAC-Bayes bounds suffer from the curse-of-dimensionality, making the practical use of PAC-Bayes training challenging on highly over-parameterized networks/models (like ResNet18 and VGG13 that outperform shallow ones in many tasks), since the over-parameterization can risk rendering the PAC-Bayes bound vacuous[16]. We summarize this challenge in (Q1).

On the other hand, the current SGD/Adam-based training procedure for neural networks requires the addition of many tricks/regularizations to achieve the best performance. To understand why these tricks/regularizations help, many recent works focused on examining them individually. For instance, it has been shown that 1) larger learning rates [12, 5], momentum [22], and smaller batch sizes [32] induce higher degrees of regularization on the Hessian or the sharpness of the loss function, subsequently yielding better generalization. 2) Techniques such as dropout [54], parameter noise injection [43], label noise [13], and batch normalization [37] serve as implicit regularizations

on the Hessian of the loss function, and the intensity of their implementation can significantly affect generalization. 3) There is evidence to suggest that the concurrent use of dropout and batch normalization may result in conflict [36]. 4) The effects on generalization by the use of mini-batch SGD/Adam can be replicated by the injection of noise into the weights [42]. 5) The generalization influence of the mini-batch in SGD can be also emulated by full-batch gradient descent, given the explicit inclusion of SGD’s implicit gradient regularization and weight clipping [20]. Despite having all these observations and explanations, it is still quite mysterious why a combination of almost all these regularizations remains essential in practice. Additionally, the process of adjusting the strengths of each regularization for different situations can be both time-consuming and heuristic. We summarize this challenge for the current training procedure in (Q2).

**Q1** : *Can PAC-Bayes training work on highly over-parameterized deep neural networks?*

**Q2** : *Can we make the training procedure less dependent on the choice of hyper-parameters and use as few regularizations/tricks as possible?*

This paper provides affirmative answers to both questions, by proposing a practical PAC-Bayes training framework. Using the framework, we show:

1. PAC-Bayes training can achieve state-of-the-art results for deep neural networks.
2. PAC-Bayes training can achieve state-of-the-art results even when the training data set is small.
3. PAC-Bayes training can be made (almost) tuning-free (only network initialization is needed) and therefore get rid of the hassle of parameter search and the use of validation data (slightly increased the amount of the training data).
4. From PAC-Bayes training, we see that among the different regularization/tricks, only weight decay and noise injections are essential: having these two are usually enough to achieve the best generalization.

## 2 Preliminaries

Throughout the paper, boldface letters denote vectors. We first introduce the basic setting of the PAC-Bayes analysis. For any supervised-learning problem, the goal is to find a good model  $\mathbf{h}$  from some hypothesis space,  $\mathbf{h} \in \mathcal{H} \subseteq \mathbb{R}^d$ , with the help of the training data  $\mathcal{S} \equiv \{z_i\}_{i=1}^m$ , and  $z_i$  is the training pair with sample  $\mathbf{x}_i$  and its label  $y_i$ . The usual assumption is that the training and test data are i.i.d. sampled from the same unknown distribution  $\mathcal{D}$ . For a given model  $\mathbf{h} \in \mathcal{H}$ , the empirical and population/generalization error are defined as:

$$\ell(\mathbf{h}; \mathcal{S}) = \frac{1}{m} \sum_{i=1}^m \ell(\mathbf{h}; z_i), \quad \ell(\mathbf{h}; \mathcal{D}) = \mathbb{E}_{\mathcal{S} \sim \mathcal{D}}(\ell(\mathbf{h}; \mathcal{S})),$$

where the loss function  $\ell(\mathbf{h}; z_i) : \mathbf{h} \mapsto \mathbb{R}^+$  measures the misfit between the true label  $y_i$  and the predicted label by the model  $\mathbf{h}$ . In particular, for the neural network setting, we have  $\ell(\mathbf{h}, z_i) = r(f_{\mathbf{h}}(\mathbf{x}_i), y_i)$ , where  $f_{\mathbf{h}}$  is the neural network parametrized by  $\mathbf{h}$ , and  $r$  is some metric of choice (e.g., MSE, cross-entropy) to measure the misfit.

PAC-Bayes bounds include a family of upper bounds on the generalization error of the following type.

**Theorem 2.1.** [38] *Assume the loss function  $\ell$  is **bounded** within the interval  $[0, C]$ . Given a fixed prior distribution  $\mathcal{P}$  over the model space  $\mathcal{H}$ , and given a scalar  $\delta \in (0, 1)$ , for any choice of i.i.d  $m$ -sized training dataset  $\mathcal{S}$  according to  $\mathcal{D}$ , and all posterior distributions  $\mathcal{Q}$  over  $\mathcal{H}$ , we have*

$$\mathbb{E}_{\mathbf{h} \sim \mathcal{Q}} \ell(\mathbf{h}; \mathcal{D}) \leq \mathbb{E}_{\mathbf{h} \sim \mathcal{Q}} \ell(\mathbf{h}; \mathcal{S}) + C \sqrt{\frac{\ln(\frac{\sqrt{2m}}{\delta}) + \text{KL}(\mathcal{Q}||\mathcal{P})}{2m}},$$

*holds with probability at least  $1 - \delta$ . Here KL stands for the Kullback-Leibler divergence.*

A PAC-Bayes bound is used to measure the gap between the expected empirical error and the expected generalization error in terms of the KL-divergence between the prior  $\mathcal{P}$  and the posterior  $\mathcal{Q}$ . It’s worth

noting that this bound holds for any data-independent prior  $\mathcal{P}$  and any posterior  $\mathcal{Q}$ , which enables one to further optimizing the bound by searching for the best posterior (known as the Gibbs-posterior). In practice, the posterior can be set to center around the trained model from data, and the prior can be selected to center around the initial model or around  $\mathbf{0}$ .

**Gap between theory and practice.** Various PAC-Bayes bounds have been proposed in the literature, with the goal of making them tight and non-vacuous. However, theoretical tightness does not necessarily equate to numerical tightness, as the former usually refers to good asymptotic rates while the latter refers merely to small values. For PAC-Bayes training, we need the latter. For instance, the bound in Theorem 2.1 is considered theoretically looser than the following one [2],

$$\mathbb{E}_{\mathbf{h} \sim \mathcal{Q}} \ell(\mathbf{h}; \mathcal{D}) \leq \mathbb{E}_{\mathbf{h} \sim \mathcal{Q}} \ell(\mathbf{h}; \mathcal{S}) + \sqrt{\mathbb{E}_{\mathbf{h} \sim \mathcal{Q}} \ell(\mathbf{h}; \mathcal{S}) \frac{\ln(\frac{2\sqrt{m}}{\delta}) + \text{KL}(\mathcal{Q}||\mathcal{P})}{m}} + \frac{\ln(\frac{2\sqrt{m}}{\delta}) + \text{KL}(\mathcal{Q}||\mathcal{P})}{m}. \quad (1)$$

as it has a smaller asymptotic rate in  $m$  when the training error gets down to 0. But if used in PAC training, the looser bound in Theorem 2.1 usually leads to better performance on both the CIFAR10 and CIFAR100 datasets as it can achieve smaller numerical values in the non-asymptotic regime of interest. This indicates that a theoretically loose PAC-Bayes bound can still be useful in practice.

**Some practical challenges faced by PAC-Bayes training.** In this section, we list some obstacles to directly using existing PAC-Bayes bound in the literature to conduct training. As the cross-entropy loss used in classification tasks is unbounded, directly applying the bound for bounded loss in Theorem 2.1 would fail.

*Bounded loss.* To use Theorem 2.1 appropriately, one can begin by converting the cross-entropy loss to a bounded version, and then apply Theorem 2.1. There are many ways to convert it to bounded loss (clipping, log-transforms), but they all tend to decrease the variance of the loss across the inputs, making the training slow. From our experience with deep neural networks, this will even cause the training accuracy to plateau at a very low level.

*Unbounded loss.* In our next attempt, we tried to use existing PAC-Bayes bounds derived for unbounded losses [23] [30]. In [23], an upper bound was derived for variables that satisfy the so-called hypothesis-dependent range condition, which is stated as  $\sup_z l(\mathbf{h}, z) \leq K(\mathbf{h})$ ,  $\forall \mathbf{h} \in \mathcal{H}$ . However, the cross entropy loss does not satisfy this condition without putting extra assumptions on the input. In [30], the author proposed PAC-Bayes bound for unbounded variables using Efron-Stein type of inequalities and obtained the following PAC-Bayes bound (adapted to our notations),

$$\mathbb{E}_{\mathbf{h} \sim \mathcal{Q}} \ell(\mathbf{h}; \mathcal{D}) \leq \mathbb{E}_{\mathbf{h} \sim \mathcal{Q}} \ell(\mathbf{h}; \mathcal{S}) + \sqrt{\frac{1}{m} \mathbb{E}_{\mathbf{h} \sim \mathcal{Q}} [\ell_1(\mathbf{h}, \mathcal{S}) + \mathbb{E}_{z' \sim \mathcal{D}} \ell(\mathbf{h}, z')] \text{KL}(\mathcal{Q}||\mathcal{P})} + \frac{1}{m},$$

where  $z_k = (\mathbf{x}_k, y_k)$  is the  $k$ th training pair, and  $z' \sim \mathcal{D}$  is a test sample drawn from the data distribution and  $\ell_1(\mathbf{h}, \mathcal{S}) := \frac{1}{m} \sum_{k=1}^m \ell(\mathbf{h}, z_k)^2$ . This bound holds for any unbounded loss with a finite second-order moment. However, it is inconvenient for PAC-Bayes training, as the term  $\mathbb{E}_{\mathbf{h} \sim \mathcal{Q}} \mathbb{E}_{z' \sim \mathcal{D}} \ell(\mathbf{h}, z')^2$  in the bound is almost as difficult to estimate as the generalization error itself empirically.

### 3 Prior art on PAC-Bayes training

The theoretical machine learning field underwent substantial evolution with the introduction of the PAC-Bayesian learning framework by McAllester [40], which built upon Shawe-Taylor’s earlier work [49]. Several works, including those by McAllester [40, 39, 41], Catoni [9, 10], Maurer [31, 38], and Germain [21], define seminal PAC-Bayes bounds. These bounds, as the one in Theorem 2.1, utilize the KL-divergence between the output posterior distribution and the prior, along with the training error, to explain generalization capabilities. Although the initial goal of creating PAC-Bayes bounds was to predict the performance of classification learning algorithms [48, 11, 21], they were soon extended to regression tasks as well [21], [38].

Recently, in the pioneering work of Dziugaite and Roy’s [16], the PAC bound was first used for training of neural networks. Specifically, McAllester’s PAC-Bayes bound [40] was used for training a shallow stochastic neural network performing binary MNIST classification with bounded 0-1 loss

and proven to be non-vacuous, i.e., exceeding the empirical test error by only a small margin with high probability. However, the performance of the proposed PAC training in this paper could not yet match that of the traditional training.

Following this work, many recent studies [33], [47], [45], [6], [44], [55] aimed to enhance the performance of PAC-Bayes training. These works focused on introducing new loss functions and expanding the applicability of PAC-Bayes bounds to a wider range of neural network architectures and datasets. For instance, Rivasplata et al. [47] introduced PBB (PAC-Bayes with BackProp), which is a self-bound algorithm that utilizes training data to learn a predictor and certify its risk through PAC-Bayes bound minimization. Their method utilizes a tighter generalization bound compared to the approach proposed by Dziugaite and Roy [16] on the MNIST dataset. However, both studies are limited to training shallow networks with binary labels on the MNIST dataset using bounded loss, which restricts their broader application to deep network training.

In another line of work, the prior and posterior are trained on separate datasets. Dziugaite et al. [15] suggested that a tighter PAC-Bayes bound could be achieved with a data-dependent prior in McAllester-type linear bounds [40]. They divide the data into two sets, using one to train the prior distribution and the other to train the posterior with the optimized prior, thus making the prior independent from the new training dataset. This, however, reduces the training data available for the posterior. Moreover, due to the use of shallow networks, the reported test accuracy didn't match the state-of-the-art performance.

The original paper by Dziugaite and Roy's [16] does not suffer from the issue of dataset splitting, as the same dataset was used for training both the prior and the posterior. Later, Dziugaite et al. [18] and Rivasplata et al [46] justified this approach by utilizing differential privacy. However, their argument only holds for priors provably satisfying the so-called  $DP(\epsilon)$ -condition in differential privacy, which limits their practical application (for more discussion please see Remark 4.2.1).

To better align with practical applications, several PAC-Bayes bounds for unbounded loss have been established [4], [3], [26], [30], [23], [46]. However, from the PAC training perspective, whether or not these theoretically tighter bounds can lead to better performance in training is still unclear. In addition, most existing PAC-Bayes training algorithms require hyper-parameter tuning, sometimes even more than vanilla SGD training, making it less feasible in practice.

In this work, we make a step forward in the PAC-Bayes training, making it more practical and demonstrating its potential to replace the normal training of neural networks in realistic settings.

## 4 Theory preparation

The proposed PAC-training framework has several key features: it includes a derivation of a relatively numerically tight PAC-bound; it includes a general theory that supports the training of the prior and the posterior simultaneously by the same training data; and it employs a layerwise prior that maintains differences of different types of layers. In this section, we will start with the necessary definitions.

**Definition 1** (Exponential moment on finite intervals). *Let  $X$  be a random variable. We call any  $K > 0$  an exponential moment bound of  $X$  on a fix interval  $[\gamma_1, \gamma_2]$  if the following holds*

$$\mathbb{E}[\exp(\gamma X)] \leq \exp(\gamma^2 K^2), \quad \forall \gamma \in [\gamma_1, \gamma_2]. \quad (2)$$

Note that this definition concurs with that of the sub-Gaussian bound when  $X$  is centered around 0 and the interval  $[\gamma_1, \gamma_2]$  is set to  $[0, \infty)$ . By using a finite interval  $[\gamma_1, \gamma_2]$ , this definition allows for a larger class of random variables to have a finite  $K$ . In particular, if  $X$  is non-negative (e.g., cross-entropy), it is known [8] that any  $X$  with a finite second-order moment will satisfy Definition 1 with a finite  $K$ . Next, to conduct the PAC-Bayes analysis, we need to extend the above definition to random variables that are parametrized by a hypothesis  $\mathbf{h} \in \mathcal{H}$ .

**Definition 2** (Exponential moment on finite intervals for unbounded variables over a hypothesis). *Let  $X(\mathbf{h})$  be a random variable parameterized by a hypothesis  $\mathbf{h} \in \mathcal{H}$ , and fix an interval  $[\gamma_1, \gamma_2]$ . Let  $\mathcal{P}_\lambda$  be some distribution over  $\mathcal{H}$  parameterized by  $\lambda \in \Lambda \subseteq \mathbb{R}^k$ , and  $\Lambda$  is the set of all possible  $\lambda$ s. Then, we call any non-negative function  $K(\lambda)$  a uniform exponential moment bound for  $X(\mathbf{h})$  over the priors  $\{\mathcal{P}_\lambda, \lambda \in \Lambda\}$  and the interval  $[\gamma_1, \gamma_2]$  if the following holds*

$$\mathbb{E}_{\mathbf{h} \sim \mathcal{P}_\lambda} \mathbb{E}[\exp(\gamma X(\mathbf{h}))] \leq \exp(\gamma^2 K^2(\lambda)), \quad \forall \gamma \in [\gamma_1, \gamma_2], \lambda \in \Lambda \subseteq \mathbb{R}^k. \quad (3)$$

Now we can start to establish the PAC-Bayes bound for the proposed PAC-Bayes training.

**Theorem 4.1.** *Given a prior distribution  $\mathcal{P}_\lambda$  parametrized by  $\lambda \in \Lambda$  over the hypothesis set  $\mathcal{H}$ . Fix some  $\lambda \in \Lambda$  and  $\delta \in (0, 1)$ . For any  $\gamma \in [\gamma_1, \gamma_2]$  and any choice of i.i.d  $m$ -sized training dataset  $\mathcal{S}$  according to  $\mathcal{D}$ , and all posterior distributions  $\mathcal{Q}$  over  $\mathcal{H}$ , we have*

$$\mathbb{E}_{\mathbf{h} \sim \mathcal{Q}} \ell(\mathbf{h}; \mathcal{D}) \leq \mathbb{E}_{\mathbf{h} \sim \mathcal{Q}} \ell(\mathbf{h}; \mathcal{S}) + \frac{1}{\gamma m} \left( \ln \frac{1}{\delta} + \text{KL}(\mathcal{Q} \parallel \mathcal{P}_\lambda) \right) + \gamma K^2(\lambda) \quad (4)$$

holds with probability at least  $1 - \delta$  when  $\ell(\mathbf{h}, \cdot)$  satisfies Definition 2 with bound  $K(\lambda)$ .

**Optimizing over the prior and posterior.** Now we select the posterior distribution as  $\mathcal{Q}_\sigma(\mathbf{h}) := \mathbf{h} + \mathcal{Q}_\sigma(0)$ , where  $\mathbf{h} \in \mathbb{R}^d$  is the current model (i.e., the network parameters) and  $\mathcal{Q}_\sigma(0)$  is a zero mean distribution parameterized by  $\sigma \in \mathbb{R}^d$ . Assuming the prior  $\mathcal{P}_\lambda$  is parameterized by  $\lambda \in \mathbb{R}^k$  ( $k \ll m, d$ ). Then for PAC training, we propose to optimize over all four variables  $\mathbf{h}$ ,  $\gamma$ ,  $\sigma$ , and  $\lambda$ .

$$(\hat{\mathbf{h}}, \hat{\gamma}, \hat{\sigma}, \hat{\lambda}) = \arg \min_{\substack{\mathbf{h}, \lambda, \sigma, \\ \gamma \in [\gamma_1, \gamma_2]}} \underbrace{\mathbb{E}_{\mathbf{h} \sim \mathcal{Q}_\sigma(\mathbf{h})} \ell(\tilde{\mathbf{h}}; \mathcal{S}) + \frac{1}{\gamma m} \left( \ln \frac{1}{\delta} + \text{KL}(\mathcal{Q}_\sigma(\mathbf{h}) \parallel \mathcal{P}_\lambda) \right) + \gamma K^2(\lambda)}_{\equiv L_{PAC}(\mathbf{h}, \gamma, \sigma, \lambda)}. \quad (\text{P})$$

Before getting into the details of the training algorithm, let us provide the theoretical error guarantee for P.

**Assumption 4.1.1** (Continuity of the KL divergence). *Let  $\mathfrak{Q}$  be a family of posterior distribution, let  $\mathfrak{P} = \{\mathcal{P}_\lambda, \lambda \in \Lambda \subseteq \mathbb{R}^k\}$  be a family of prior distributions parameterized by a  $k$ -dimensional variable vector  $\lambda \in \mathbb{R}^k$ . We say the posterior family  $\mathfrak{Q}$  is continuous with respect to the parameterization of the prior under a metric  $\|\cdot\|$  defined on  $\Lambda$ , if there exist  $\varepsilon_0 > 0$  and a non-decreasing function  $\eta_1(x) : \mathbb{R}_+ \rightarrow \mathbb{R}_+$  such that for any  $0 < \varepsilon < \varepsilon_0$  and  $\lambda, \tilde{\lambda} \in \Lambda$ ,  $\|\tilde{\lambda} - \lambda\| < \varepsilon$ , it holds that*

$$|\text{KL}(\mathcal{Q} \parallel \mathcal{P}_\lambda) - \text{KL}(\mathcal{Q} \parallel \mathcal{P}_{\tilde{\lambda}})| \leq \eta_1(\|\lambda - \tilde{\lambda}\|),$$

for any  $\mathcal{Q} \in \mathfrak{Q}$ .

**Assumption 4.1.2** (Continuity of the moment bound). *Let the  $K(\lambda)$  be as defined in Definition 2. Assume it is continuous with respect to the parameter  $\lambda$  of the prior in the sense that there exists a non-decreasing function  $\eta_2(x) : \mathbb{R}_+ \rightarrow \mathbb{R}_+$  such that*

$$|K^2(\lambda) - K^2(\tilde{\lambda})| \leq \eta_2(\|\lambda - \tilde{\lambda}\|), \quad \forall \lambda, \tilde{\lambda} \in \Lambda.$$

**Theorem 4.2.** *Let  $n(\varepsilon) := \mathcal{N}(\Lambda, \|\cdot\|, \varepsilon)$  be the covering number of the set  $\Lambda$  of the prior parameters. Under Assumption 4.1.1 and Assumption 4.1.2, the following inequality holds for the minimizer  $(\hat{\mathbf{h}}, \hat{\gamma}, \hat{\sigma}, \hat{\lambda})$  of (P) with probability as least  $1 - \varepsilon$ :*

$$\begin{aligned} \mathbb{E}_{\mathbf{h} \sim \mathcal{Q}_{\hat{\sigma}}(\hat{\mathbf{h}})} \ell(\mathbf{h}; \mathcal{D}) &\leq \mathbb{E}_{\mathbf{h} \sim \mathcal{Q}_{\hat{\sigma}}(\hat{\mathbf{h}})} \ell(\mathbf{h}; \mathcal{S}) + \frac{1}{\hat{\gamma} m} \left[ \ln \frac{n(\varepsilon)}{\varepsilon} + \text{KL}(\mathcal{Q}_{\hat{\sigma}}(\hat{\mathbf{h}}) \parallel \mathcal{P}_{\hat{\lambda}}) \right] + \hat{\gamma} K^2(\hat{\lambda}) + \eta \\ &= L_{PAC}(\hat{\mathbf{h}}, \hat{\gamma}, \hat{\sigma}, \hat{\lambda}) + \eta + \frac{\ln(n(\varepsilon))}{\hat{\gamma} m} \end{aligned} \quad (5)$$

holds for any  $\varepsilon, \varepsilon > 0$ , where  $\eta = (\frac{1}{\gamma_1 m} + \gamma_2)(\eta_1(\varepsilon) + \eta_2(\varepsilon))$ .

Since  $(\hat{\mathbf{h}}, \hat{\gamma}, \hat{\sigma}, \hat{\lambda})$  is the minimizer of  $L_{PAC}(\mathbf{h}, \gamma, \sigma, \lambda)$ , the first term on the right-hand side of (5) is guaranteed to be the smallest possible. In applications, we need to ensure the correction terms (i.e., the second and third terms) are small. This can usually be achieved by selecting a relatively small  $k$ , the dimension of the prior parameter  $\lambda$ , compared to the dataset size. More discussions can be found in the next section.

**Remark 4.2.1.** *Theoretical justification for the use of data-dependent prior was previously provided in [46] and [18] by using differential privacy. However, the requirement for the prior to be differentially private restricts its application to generalization settings. In particular, the prior encountered in this paper, since it is only implicitly defined as a solution to a non-convex optimization problem with no good closed-form expression, the condition for differential privacy is hard to be verified. In contrast, Theorem 4.2 holds for arbitrary data-dependent priors.*

## 5 PAC-Bayes training algorithm

### 5.1 Gaussian prior and posterior

In our PAC training, we use Gaussian distributions for both the prior and posterior. We set the prior distribution to be centered around the initialization of the neural network  $\mathbf{h}_0$  (as suggested by [17]), having independent entries and with a scalar variance for all the weights in one layer (different from [17]). For a  $k$ -layer network, the prior is written as  $\mathcal{P}_\lambda(\mathbf{h}_0)$ , where  $\lambda \in \mathbb{R}_+^k$  is the vector containing the variance for each layer. The set of all such priors is denoted by  $\mathfrak{P} := \{\mathcal{P}_\lambda(\mathbf{h}_0), \lambda \in \Lambda\}$ . We select the posterior distribution to be centered around the trained model  $\mathbf{h}$ , with independent anisotropic variance. Specifically, for a network with  $d$  trainable parameters, the posterior is set to  $\mathcal{Q}_\sigma(\mathbf{h}) := \mathcal{N}(\mathbf{h}, \text{diag}(\sigma))$ , where  $\mathbf{h}$  is the mean and  $\sigma \in \mathbb{R}_+^d$  is the vector containing the variance for each trainable parameter. The set of all posteriors is  $\mathfrak{Q} := \{\mathcal{Q}_\sigma(\mathbf{h}), \sigma \in \Sigma, \mathbf{h} \in \mathcal{H}\}$ , and the KL divergence between such prior and posterior is

$$\text{KL}(\mathcal{Q}_\sigma(\mathbf{h})||\mathcal{P}_\lambda(\mathbf{h}_0)) = \frac{1}{2} \sum_{i=1}^k \left[ -\mathbf{1}_{d_i}^\top \ln(\sigma_i) + d_i(\ln(\lambda_i) - 1) + \frac{\|\sigma_i\|_1 + \|(\mathbf{h} - \mathbf{h}_0)_i\|^2}{\lambda_i} \right], \quad (6)$$

where  $\sigma_i, (\mathbf{h} - \mathbf{h}_0)_i$  are vectors denoting the variances and weights for the  $i$ -th layer, respectively, and  $\lambda_i$  is the scalar variance for the  $i$ -th layer.  $d_i = \dim(\sigma_i)$ , and  $\mathbf{1}_{d_i}$  denotes an all-ones vector of length  $d_i$ . Substituting the Gaussian prior and posterior into Theorem 4.2 gives the following corollary.

**Corollary 5.0.1.** *Assume the parameter sets of priors and posteriors are both bounded,  $\mathcal{H} := \{\mathbf{h} \in \mathbb{R}^d : \|\mathbf{h}\|_2 \leq M\}$ ,  $\Sigma := \{\sigma \in \mathbb{R}_+^d : \|\sigma\|_1 \leq T\}$ ,  $\Lambda := \{\lambda \in [e^{-a}, e^b]^k\}$ , and assume  $\ell(\mathbf{h}, \cdot)$  satisfies Definition 2 with bound  $K(\lambda)$  and  $K^2(\lambda)$  is Lipschitz continuous with Lipschitz constant  $C_K$ . Then with high probability, the PAC-Bayes bound for the minimizer of (P) has the form*

$$\mathbb{E}_{h \sim \mathcal{Q}_{\hat{\sigma}}(\hat{\mathbf{h}})} \ell(\mathbf{h}; \mathcal{D}) \leq L_{PAC}(\hat{\mathbf{h}}, \hat{\gamma}, \hat{\sigma}, \hat{\lambda}) + \eta,$$

where  $\eta = \frac{k}{\gamma_1 m} \left( 1 + \ln \frac{C(C_K + L(d))(b+a)\gamma_1 m}{2k} \right)$ ,  $C = \frac{1}{\gamma_1 m} + \gamma_2$ ,  $L(d) = \frac{1}{2} \max\{d, e^a(2M + T)\}$

**Remark 5.0.1.** *The boundedness of the parameter sets in the assumption of Corollary 5.0.1 can be guaranteed by clipping the variables during training (usually not needed if the training dataset is large), and the Lipschitz continuity assumption on  $K(\lambda)$  can be verified numerically from data.*

Again since  $(\hat{\mathbf{h}}, \hat{\gamma}, \hat{\sigma}, \hat{\lambda})$  is the minimizer of  $L_{PAC}(\mathbf{h}, \gamma, \sigma, \lambda)$ , the first term in the bound is guaranteed to be small. The correction term  $\eta$  would also be small as long as  $k$  is much smaller than  $m$ , which means the trainable parameters in the prior distribution has to be much smaller than the number of training samples. For the large CIFAR10/100 dataset [29] with  $m = 5 \times 10^4$ , the correction term would be very small even with a deep CNN<sup>1</sup>. But for small graph datasets, such as PubMed [7] where  $m = 60$ , the correction term could become large. If this happens, then we need to set a smaller bound for the parameter sets of the prior and the posterior distributions and use clipping to enforce the parameters falling into this range during training. More discussions about details are available in the appendix (Sec. C, D).

**Scalar prior.** Scalar prior is a special case of the layerwise prior by setting all entries of  $\lambda$  to be equal, for which the KL divergence reduces to

$$\text{KL}(\mathcal{Q}_\sigma(\mathbf{h})||\mathcal{P}_\lambda(\mathbf{h}_0)) = \frac{1}{2} \left[ -\mathbf{1}_d^\top \ln(\sigma) + d(\ln(\lambda) - 1) + \frac{1}{\lambda} (\|\sigma\|_1 + \|\mathbf{h} - \mathbf{h}_0\|^2) \right]. \quad (7)$$

When the data size is small, PAC-Bayes training with scalar prior may deliver better performance than the layerwise one by limiting the number of trainable parameters in the prior to one.

### 5.2 Estimating $K(\lambda)$ and $C_K$

In order to optimize  $L_{PAC}$ , we first need to estimate the function  $K(\lambda)$ . For the PAC-Bayes bound to be effective, the value of  $K(\lambda)$  cannot be too large. In fact, this is why we made  $K$  a function of  $\lambda$

<sup>1</sup>In all our experiments for various neural networks, we set  $\gamma_1 = 0.5$  and  $\gamma_2 = 10$ .

and only requires the inequality to hold on a finite interval in Definition 2, as otherwise, the estimated  $K$  will be too large. In practice, we estimate  $K(\lambda)$  using linear interpolation: first for a discrete set,  $\{\lambda_1, \dots, \lambda_s\} \subseteq \Lambda^2$ , we estimate the corresponding  $K_1, \dots, K_s$  using the empirical version of (2), that is for any  $i = 1, \dots, s$ , we solve

$$\begin{aligned} \hat{K}_i &= \arg \min_{K > 0} K \\ \text{s.t. } \exp(\gamma^2 K^2) &\geq \frac{1}{nm} \sum_{l=1}^n \sum_{j=1}^m \exp(\gamma(\ell(\mathbf{h}_l; \mathcal{S}) - \ell(\mathbf{h}_l; z_j))) \quad \forall \gamma \in [\gamma_1, \gamma_2], \end{aligned} \quad (8)$$

for  $K(\lambda_i)$ , where  $\mathbf{h}_l \sim \mathcal{P}_{\lambda_i}(\mathbf{h}_0)$ ,  $l = 1, \dots, n$ , are samples from the prior distribution and are fixed when solving (8). The minimizer  $\hat{K}_i$  is found using a bisection search. From the pairs  $(\lambda_i, K(\lambda_i))$ , we construct  $K(\lambda)$  using function interpolation, which then allows us to compute the derivative of  $K(\lambda)$  when optimizing the PAC-Bayes loss. Notably, since for each fixed  $\lambda_i$ , the prior is independent of the data, this procedure of estimating  $K(\lambda)$  can be carried out before training. Algorithm 1 summarizes the procedure of computing  $K(\lambda)$  before training. Moreover, if one wants to apply Corollary 5.0.1 to estimate the final prediction error of the PAC training, it is sufficient to estimate the Lipschitz constant  $C_K$  also from the interpolated function.

---

**Algorithm 1** Compute  $K(\lambda)$  given a set of query priors

---

**Input:**  $\gamma_1$  and  $\gamma_2$ ,  $s$  query prior variances  $\mathcal{V} = \{\lambda_i \in \Lambda \subseteq \mathbb{R}^k, i = 1, \dots, s\}$ , the initial neural network weight  $\mathbf{h}_0$ , the training dataset  $\mathcal{S} = \{z_i\}_{i=1}^m$ , model sampling time  $n = 10$

**Output:** the piece-wise linear interpolation  $\tilde{K}(\lambda)$  for  $K(\lambda)$

**for**  $\lambda_i \in \mathcal{V}$  **do**

Set up a discrete grid  $\Gamma$  for the interval  $[\gamma_1, \gamma_2]$  of  $\gamma$ .

**for**  $l = 1 : n$  **do**

Sampling weights from the Gaussian distribution  $\mathbf{h}_l \sim \mathcal{N}(\mathbf{h}_0, \lambda_i)$

Use  $\mathbf{h}_l$ ,  $\Gamma$  and  $\mathcal{S}$  to compute one term in the sum in (8)

**end for**

Solve  $\hat{K}_i$  using (8)

**end for**

Fit a piece-wise linear function  $\tilde{K}(\lambda)$  to the data  $\{(\lambda_i, \hat{K}_i)\}_{i=1}^s$

---

More details about the  $K$  estimation for the layer-wise prior are in the appendix (Sec. A).

### 5.3 PAC-Bayes bound minimization (Auto-tune)

Like [17], we use the Adam optimizer to optimize the model, the prior and the posterior, except that 1) we also optimize  $K(\lambda)$  over the prior variance; 2) we allow the loss to be unbounded; and 3) we allow the network to be deep by using the layer-wised prior.

**Tuning-free PAC-Bayes training.** Algorithm 2 and 3 describe the PAC-Bayes training procedure with scalar and layerwise prior. Here, we directly minimize  $L_{PAC}$  using Adam. Although there are many input parameters to be specified, their value can be largely fixed across very different settings, and therefore not much actual tuning is needed. The only essential input is the initial model  $\mathbf{h}_0$ , for which we use the default Kaiming initialization [25] as in normal training. The loss function is defined as Equation (P) with the KL term defined in (6). When everything else is fixed,  $\gamma \in [\gamma_1, \gamma_2]$  has a closed-form solution,

$$\gamma^* = \min \left\{ \max \left\{ \gamma_1, \frac{1}{K} \sqrt{\frac{\ln \frac{1}{\delta} + \text{KL}(\mathcal{Q}_{\sigma}(\mathbf{h}) || \mathcal{P}_{\lambda}(\mathbf{h}_0))}{m}} \right\}, \gamma_2 \right\}. \quad (9)$$

So, we only need to perform gradient updates on the other three variables,  $\mathbf{h}$ ,  $\sigma$ ,  $\lambda$ . We would like to comment that as PAC-Bayes training involves more trainable parameters, the optimization inevitably

---

<sup>2</sup>Note that with a little ambiguity, the  $\lambda_i$  here has a different meaning from that in (6)), here  $\lambda_i$  means the  $i$ th element in the discrete set, whereas in (6),  $\lambda_i$  means the  $i$ th element in  $\lambda$ .

---

**Algorithm 2** Tuning-free PAC-Bayes training (scalar prior)

---

**Input:** initial model  $\mathbf{h}_0 \in \mathbb{R}^d$ ,  $T_1 = 500$ ,  $\lambda_1 = e^{-7}$ ,  $\lambda_2 = 1$ ,  $\gamma_1 = 0.5$ ,  $\gamma_2 = 10$

**Output:** trained model  $\hat{\mathbf{h}}$ , posterior noise level  $\hat{\sigma}$

$\mathbf{h} \leftarrow \mathbf{h}_0$ ,  $\mathbf{v} \leftarrow \mathbf{1}_d \cdot \log(\frac{1}{d} \|\mathbf{h}_0\|_1)$ ,  $b \leftarrow \log(\frac{1}{d} \|\mathbf{h}_0\|_1)$

Obtain the estimated  $\hat{K}(\lambda)$  with  $\Lambda = [\lambda_1, \lambda_2]$  using (8) (Algorithm 1)

**for** epoch = 1 :  $T_1$  **do** ▷ Stage 1

**for** sampling one batch  $s$  from  $\mathcal{S}$  **do**

$\lambda \leftarrow \exp(b)$ ,  $\boldsymbol{\sigma} \leftarrow \exp(\mathbf{v})$

$\mathcal{P}_\lambda \leftarrow \mathcal{N}(\mathbf{h}_0; \lambda I_d)$ ,  $\mathcal{Q}_{\boldsymbol{\sigma}}(\mathbf{h}) \leftarrow \mathbf{h} + \mathcal{N}(\mathbf{0}; \text{diag}(\boldsymbol{\sigma}))$

    Draw one  $\tilde{\mathbf{h}} \sim \mathcal{Q}_{\boldsymbol{\sigma}}(\mathbf{h})$  and evaluate  $\ell(\tilde{\mathbf{h}}; \mathcal{S})$ , ▷ Stochastic version of  $\mathbb{E}_{\tilde{\mathbf{h}} \sim \mathcal{Q}_{\boldsymbol{\sigma}}(\mathbf{h})} \ell(\tilde{\mathbf{h}}; \mathcal{S})$

    Compute the KL-divergence as (7)

    Compute  $\gamma$  as (9)

    Compute the loss function  $\mathcal{L}$  as  $L_{PAC}$  in (P)

$b \leftarrow b + \eta \frac{\partial \mathcal{L}}{\partial b}$ ,  $\mathbf{v} \leftarrow \mathbf{v} + \eta \frac{\partial \mathcal{L}}{\partial \mathbf{v}}$ ,  $\mathbf{h} \leftarrow \mathbf{h} + \eta \frac{\partial \mathcal{L}}{\partial \mathbf{h}}$  ▷ Update all parameters

**end for**

**end for**

$\hat{\sigma} \leftarrow \exp(\mathbf{v})$  ▷ Fix the noise level from now on

**while** not converge **do** ▷ Stage 2

**for** sampling one batch  $s$  from  $\mathcal{S}$  **do**

    Draw one sample  $\tilde{\mathbf{h}} \sim \mathcal{Q}_{\hat{\sigma}}(\mathbf{h})$  and evaluate  $\ell(\tilde{\mathbf{h}}; \mathcal{S})$  as  $\tilde{\mathcal{L}}$ , ▷ Noise injection

$\mathbf{h} \leftarrow \mathbf{h} + \eta \frac{\partial \tilde{\mathcal{L}}}{\partial \mathbf{h}}$  ▷ Update model parameters

**end for**

**end while**

$\hat{\mathbf{h}} \leftarrow \mathbf{h}$

---

becomes harder but we found that it is still quite manageable. More details about the implementation and discussions can be found in the appendix (Sec. 8, B).

**The second stage of training.** In many cases, the PAC-Bayes training does not allow the training accuracy to reach nearly 100%, due to the existence of the KL term. However, for many classification tasks, a high training accuracy is usually essential for good testing accuracy. Therefore, we add a second stage to the PAC-Bayes training stage (Stage 1) to make the training converge. Specifically, in Stage 2, we continue to update the model by minimizing only  $\mathbb{E}_{\mathbf{h} \sim \mathcal{Q}_{\hat{\sigma}}} \ell(\mathbf{h}; \mathcal{S})$  over  $\mathbf{h}$  using Adam and keep all other variables fixed to the solution found by Stage 1, which is essentially a stochastic gradient update with noise injection whose level has been learned from Stage 1.

**Evaluation/Prediction.** The bound derived in the PAC-Bayes theorems pertains to the Bayesian predictor, which is constructed by averaging predictions over the posterior distribution  $\mathcal{Q}_{\hat{\sigma}}(\mathbf{h})$ . In practice, implementing this Bayesian predictor involves evaluating the new input across multiple models sampled from the posterior distribution, and then employing an average or voting procedure to obtain a final prediction. In this paper, however, we propose using a simple deterministic predictor that relies solely on the final trained model for making predictions. This approach offers several advantages. Firstly, it eliminates the need for multiple model evaluations. Additionally, this deterministic predictor has the potential to enhance performance based on the following intuition.

Recall that for any  $\mathbf{h} \in \mathbb{R}^d$  and  $\boldsymbol{\sigma} \in \mathbb{R}_+^d$ , we used  $\mathcal{Q}_{\boldsymbol{\sigma}}(\mathbf{h})$  to denote the multivariate normal distribution with mean  $\mathbf{h}$  and covariance matrix  $\text{diag}(\boldsymbol{\sigma})$ . Now let us Taylor expand the left-hand side of the PAC-Bayes bound:

$$\begin{aligned}
\mathbb{E}_{\mathbf{h} \sim \mathcal{Q}_{\hat{\sigma}}(\hat{\mathbf{h}})} \ell(\mathbf{h}; \mathcal{D}) &= \mathbb{E}_{\Delta \mathbf{h} \sim \mathcal{Q}_{\hat{\sigma}}(0)} \ell(\hat{\mathbf{h}} + \Delta \mathbf{h}; \mathcal{D}) \\
&\approx \ell(\hat{\mathbf{h}}; \mathcal{D}) + \mathbb{E}_{\Delta \mathbf{h} \sim \mathcal{Q}_{\hat{\sigma}}(0)} (\ell(\hat{\mathbf{h}}; \mathcal{D}) \Delta \mathbf{h} + \frac{1}{2} \Delta \mathbf{h}^\top \nabla^2 \ell(\hat{\mathbf{h}}; \mathcal{D}) \Delta \mathbf{h}) \\
&= \ell(\hat{\mathbf{h}}; \mathcal{D}) + \frac{1}{2} \text{Tr}(\text{diag}(\boldsymbol{\sigma}) \nabla^2 \ell(\hat{\mathbf{h}}; \mathcal{D})) \geq \ell(\hat{\mathbf{h}}; \mathcal{D}).
\end{aligned} \tag{10}$$

Recall here  $\hat{\mathbf{h}}$  and  $\hat{\sigma}$  are the minimizers of the PAC-Bayes loss, obtained by solving the optimization problem (P). Equation (10) states that the deterministic predictor has a smaller prediction error than

---

**Algorithm 3** Tuning-free PAC-Bayes training (layer-wise prior)

---

**Input:** initial model  $\mathbf{h}_0 \in \mathbb{R}^d$ , the number of layers  $k$ ,  $T_1$ ,  $\lambda_1 = e^{-7}$ ,  $\lambda_2 = 1$ ,  $\gamma_1 = 0.5$ ,  $\gamma_2 = 10$   
**Output:** trained model  $\hat{\mathbf{h}}$ , posterior noise level  $\hat{\sigma}$

$\mathbf{h} \leftarrow \mathbf{h}_0$ ,  $\mathbf{v} \leftarrow \mathbf{1}_d \cdot \log(\frac{1}{d} \sum_{i=1}^d |\mathbf{h}_{0,i}|)$ ,  $\mathbf{b} \leftarrow \mathbf{1}_k \cdot \log(\frac{1}{d} \sum_{i=1}^d |\mathbf{h}_{0,i}|)$  ▷ Initialization  
Obtain the estimated  $\tilde{K}(\tilde{\lambda})$  with  $\Lambda = [\lambda_1, \lambda_2]^k$  using (8) and Sec. A  
**for** epoch = 1 :  $T_1$  **do** ▷ Stage 1  
  **for** sampling one batch  $s$  from  $\mathcal{S}$  **do**  
     $\lambda \leftarrow \exp(\mathbf{b})$ ,  $\sigma \leftarrow \exp(\mathbf{v})$   
    Construct the covariance of  $\mathcal{P}_\lambda$  from  $\lambda$  ▷ Setting the variance of the weights in layer- $i$  all to the scalar  $\lambda(i)$   
    Draw one  $\tilde{\mathbf{h}} \sim \mathcal{Q}_\sigma(\mathbf{h})$  and evaluate  $\ell(\tilde{\mathbf{h}}; \mathcal{S})$ , ▷ Stochastic version of  $\mathbb{E}_{\tilde{\mathbf{h}} \sim \mathcal{Q}_\sigma(\mathbf{h})} \ell(\tilde{\mathbf{h}}; \mathcal{S})$   
    Compute the KL-divergence as (6)  
    Compute  $\gamma$  as (9)  
    Compute the loss function  $\mathcal{L}$  as  $L_{PAC}$  in (P)  
     $\mathbf{b} \leftarrow \mathbf{b} + \eta \frac{\partial \mathcal{L}}{\partial \mathbf{b}}$ ,  $\mathbf{v} \leftarrow \mathbf{v} + \eta \frac{\partial \mathcal{L}}{\partial \mathbf{v}}$ ,  $\mathbf{h} \leftarrow \mathbf{h} + \eta \frac{\partial \mathcal{L}}{\partial \mathbf{h}}$  ▷ Update all parameters  
  **end for**  
**end for**  
 $\hat{\sigma} \leftarrow \exp(\mathbf{v})$  ▷ Fix the noise level from now on  
**while** not converge **do** ▷ Stage 2  
  **for** sampling one batch  $s$  from  $\mathcal{S}$  **do**  
    Draw one sample  $\tilde{\mathbf{h}} \sim \mathcal{Q}_{\hat{\sigma}}(\mathbf{h})$  and evaluate  $\ell(\tilde{\mathbf{h}}; \mathcal{S})$  as  $\tilde{\mathcal{L}}$ , ▷ Noise injection  
     $\mathbf{h} \leftarrow \mathbf{h} + \eta \frac{\partial \tilde{\mathcal{L}}}{\partial \mathbf{h}}$  ▷ Update model parameters  
  **end for**  
**end while**  
 $\hat{\mathbf{h}} \leftarrow \mathbf{h}$

---

the Bayesian predictor. However, note that the last inequality in (10) is derived under the assumption that the term  $\nabla^2 \ell(\hat{\mathbf{h}}, \mathcal{D})$  is positive-semidefinite. This is a reasonable assumption as  $\hat{\mathbf{h}}$  is the local minimizer of the PAC-Bayes loss and the PAC-Bayes loss is close to the population loss when the number of samples is large. Nevertheless, since this assumption does not hold for all cases, the presented argument can only serve only as an intuition that shows the potential benefits of using the deterministic predictor.

**Regularizations in the PAC-Bayes loss:** Plugging the KL divergence formula (6) into (P), we can see that in the case of the Gaussian prior, the PAC-Bayes loss is nothing but the original training loss augmented by a noise injection and a weight decay, except that the weight decay term is now centered at  $\mathbf{h}_0$  instead of  $\mathbf{0}$ , the coefficients in front of the weight decay change from layer to layer, and the noise injection has anisotropic variances. Since many factors in normal training, such as mini-batch and dropout, enhance generalization by some sort of noise injection, it is not surprising that they can be substituted by just the well-calibrated noise injection mechanism in PAC-Bayes training.

## 6 Experiments

**Evaluation on deep convolution neural networks:** We test the proposed method on the CIFAR10 and CIFAR100 datasets with *no data augmentation* on various popular deep neural networks including ResNet18, ResNet34 [50], VGG13 and VGG19 [34], and DenseNet121 [27] by comparing its performance with the normal training by SGD and Adam with various regularizations (which we call baseline). The baseline training involves a grid search of hyper-parameters, including the optimizer (SGD/Adam/AdamW), momentum for SGD (0.3, 0.6, 0.9), learning rates ( $1e-3$ ,  $5e-3$ ,  $1e-2$ ,  $5e-2$ ,  $1e-1$ ,  $2e-1$ ), weight decay ( $1e-4$ ,  $5e-4$ ,  $1e-3$ ,  $5e-3$ ,  $1e-2$ ), and noise injection ( $5e-4$ ,  $1e-3$ ,  $5e-3$ ,  $1e-2$ ), thus it is quite time-consuming. To make this search possible, we adjusted one hyper-parameter at a time while keeping the others fixed. To determine the optimal hyper-parameter for a variable, we used the mean testing accuracy of the last five epochs. We then used this selected hyper-parameter to tune the next one. We only applied noise injection to Adam/AdamW, as it sometimes causes instability with SGD. The best learning rate for Adam and

Table 1: Testing accuracy of convolution neural networks on C10 (CIFAR10) and C100 (CIFAR100). "scalar" and "layer" denote the PAC-Bayes training (Auto-tune) with scalar and layer-wised prior.

(a) VGG13			(b) VGG19			(c) Resnet18			(d) Resnet34			(e) DenseNet121		
C10		C100	C10		C100	C10		C100	C10		C100	C10		C100
SGD	90.2	66.9	SGD	90.2	64.5	SGD	89.9	64.0	SGD	90.0	70.3	SGD	91.8	74.0
Adam	88.5	63.7	Adam	89.0	58.8	Adam	87.5	61.6	Adam	87.9	59.5	Adam	91.2	70.0
AdamW	88.4	61.8	AdamW	89.0	62.3	AdamW	87.9	61.4	AdamW	88.3	59.9	AdamW	91.5	70.1
scalar	88.7	67.2	scalar	89.2	61.3	scalar	88.0	68.8	scalar	89.6	69.5	scalar	91.2	71.4
layer	89.7	67.1	layer	90.5	62.3	layer	89.3	68.9	layer	90.9	69.9	layer	91.5	72.2

Table 2: The results of large batch sizes on the testing accuracy of CNNs on C10 (CIFAR10) and C100 (CIFAR100). The number in (·) indicates how much the results differ from using a small batch size of (128). "scalar" and "layer" denote the PAC-Bayes training (Auto-tune) with scalar and layer-wised prior. The best results are **highlighted**.

(a) VGG13			(b) ResNet18			(c) ResNet34		
C10		C100	C10		C100	C10		C100
SGD	87.7 (-2.5)	60.1 (-6.8)	SGD	85.4 (-4.5)	61.5 (-2.6)	SGD	87.0 (-3.0)	61.5 (-8.8)
Adam	<b>90.7</b> (+2.2)	66.2 (+2.5)	Adam	87.7 (+0.2)	65.4 (+3.8)	Adam	89.5 (+1.6)	67.1 (+7.6)
AdamW	87.2 (-1.1)	61.0 (-0.8)	AdamW	84.9 (-2.9)	58.9 (-2.5)	AdamW	86.8 (-1.5)	58.8 (-1.1)
scalar	88.9 (0.2)	66.0 (-1.2)	scalar	88.9 (0.9)	68.7 (-0.1)	scalar	90.2 (0.6)	67.5 (-2.0)
layer	89.4 (-0.3)	<b>67.1</b> (-0.0)	layer	<b>89.2</b> (-0.1)	<b>69.3</b> (+0.3)	layer	<b>90.6</b> (-0.3)	<b>69.1</b> (-0.8)

AdamW is the same since weight decay is the only difference between the two optimizers. We set batch size as 128, since from the literature, it usually gives the best performance. Finally, 38 searches were conducted for each baseline model on one dataset. The testing accuracy for the optimally-tuned baseline and a single run of the Tuning-free PAC-Bayes training are presented in Table 1. Since there is no published validation dataset in the CIFAR10 and CIFAR100, we (unfairly) used the test dataset to tune the hyperparameters for the baseline, which would make the reported performance of the baseline slightly inflated compared to its actual performance. Nevertheless, the testing accuracy of our method with scalar and layer-wised prior match the best testing accuracy of baselines. There is no grid search for our PAC-Bayes training, and we use Adam as the optimizer and use the learning rate as  $1e-4$  for all models. To provide more details, we have plotted all the searched results for the baseline for VGG13, ResNet34, and DenseNet121 on CIFAR100 in Figure 1. The plotted results are sorted in ascending order based on their testing accuracy. The figure shows that our proposed training algorithms are better than most searched settings.

**Extra stability to the batch size:** Additionally, we find that the result of the tuning-free PAC training is insensitive to the batch size. Table 2 shows that changing the batch size from 128 to 2048 for VGG13 and ResNet18 does not decrease the performance of the PAC-Bayes training as much as it does for the normal training. Despite not requiring exhaustive tuning, our proposed tuning-free algorithms match the best testing accuracy of the baseline with a much larger batch size. This observation enables using large batch sizes for the PAC training to accelerate the convergence. Besides the batch size, our proposed method is also insensitive to the learning rate. Please refer to the appendix (Sec. H.1, and H.2) for more details.

**Evaluation on graph neural networks:** To demonstrate the robustness of the proposed PAC training algorithm across different network architectures, we also test it on the graph neural networks. Moreover, the number of training samples for node classification tasks is generally much smaller than CIFAR10/100, allowing us to examine the performance of the algorithm in the data scarcity setting. Unlike CNNs, the GNN baselines find their best performance with AdamW optimizer and with dropout turned on, while the proposed PAC-Bayes training algorithm stays the same as in the CNN setting. To ensure the best results of the baseline, we fine-tuned the learning rate

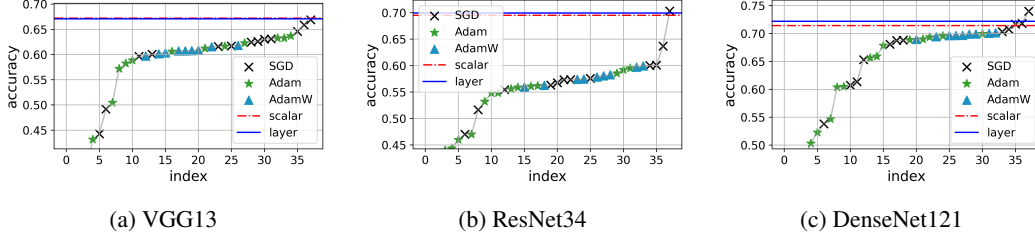


Figure 1: Sorted testing accuracy of CIFAR100. "scalar" and "layer" represent the tuning-free PAC-Bayes training with the scalar and layerwise prior.

Table 3: Testing accuracy of GNNs with different training settings. "+val" denotes combining validation nodes to training, where the best hyper-parameters selected from "AdamW" is used in "AdamW+val". The highest testing accuracy is **highlighted**.

		CoraML	Citeseer	Pubmed	Cora	DBLP
GCN	AdamW	81.9 $\pm$ 1.8	84.3 $\pm$ 1.2	78.3 $\pm$ 2.3	58.6 $\pm$ 0.6	71.6 $\pm$ 1.2
	scalar	83.5 $\pm$ 1.1	84.0 $\pm$ 1.4	78.8 $\pm$ 2.2	59.6 $\pm$ 1.0	74.9 $\pm$ 1.6
	AdamW+val	85.7 $\pm$ 0.7	<b>90.3<math>\pm</math>0.4</b>	<b>85.0<math>\pm</math>0.6</b>	60.7 $\pm$ 0.7	<b>80.6<math>\pm</math>1.4</b>
	scalar+val	<b>86.1<math>\pm</math>0.7</b>	90.0 $\pm$ 0.4	84.9 $\pm$ 0.8	<b>62.0<math>\pm</math>0.4</b>	80.5 $\pm$ 0.6
GAT	AdamW	81.7 $\pm$ 1.0	85.3 $\pm$ 0.7	78.1 $\pm$ 2.1	60.1 $\pm$ 0.8	75.5 $\pm$ 2.3
	scalar	81.6 $\pm$ 1.2	85.0 $\pm$ 1.1	77.5 $\pm$ 2.4	58.9 $\pm$ 0.9	75.9 $\pm$ 1.6
	AdamW+val	85.7 $\pm$ 1.0	<b>90.8<math>\pm</math>0.3</b>	84.0 $\pm$ 0.4	<b>63.5<math>\pm</math>0.4</b>	<b>81.8<math>\pm</math>0.6</b>
	scalar+val	<b>85.9<math>\pm</math>0.8</b>	90.6 $\pm$ 0.5	<b>84.4<math>\pm</math>0.5</b>	60.9 $\pm$ 0.6	81.0 $\pm$ 0.5
SAGE	AdamW	80.6 $\pm$ 1.4	84.5 $\pm$ 1.3	75.7 $\pm$ 2.4	55.6 $\pm$ 0.6	71.8 $\pm$ 1.6
	scalar	80.8 $\pm$ 1.4	83.7 $\pm$ 1.3	74.3 $\pm$ 2.5	55.5 $\pm$ 1.6	73.6 $\pm$ 1.3
	AdamW+val	85.7 $\pm$ 0.5	<b>90.5<math>\pm</math>0.5</b>	83.5 $\pm$ 0.4	60.6 $\pm$ 0.5	<b>80.7<math>\pm</math>0.6</b>
	scalar+val	<b>86.5<math>\pm</math>0.5</b>	90.0 $\pm$ 0.5	<b>84.4<math>\pm</math>0.6</b>	<b>61.2<math>\pm</math>0.2</b>	79.9 $\pm$ 0.5
APPNP	AdamW	83.5 $\pm$ 1.3	85.3 $\pm$ 1.1	80.0 $\pm$ 2.4	59.8 $\pm$ 0.8	77.0 $\pm$ 2.2
	scalar	83.7 $\pm$ 1.1	85.2 $\pm$ 1.3	79.3 $\pm$ 3.5	60.0 $\pm$ 0.7	77.4 $\pm$ 2.6
	AdamW+val	86.6 $\pm$ 0.7	<b>91.0<math>\pm</math>0.4</b>	85.1 $\pm$ 0.5	62.5 $\pm$ 0.4	80.6 $\pm$ 2.8
	scalar+val	<b>87.1<math>\pm</math>0.6</b>	90.4 $\pm$ 0.5	<b>85.7<math>\pm</math>0.4</b>	<b>63.5<math>\pm</math>0.4</b>	<b>81.8<math>\pm</math>0.5</b>

( $1e-3$ ,  $5e-3$ ,  $1e-2$ ), weight decay ( $0$ ,  $1e-2$ ,  $1e-3$ ,  $1e-4$ ), noise injection ( $0$ ,  $1e-3$ ,  $1e-2$ ,  $1e-3$ ), and dropout ( $0$ ,  $0.4$ ,  $0.8$ ). We follow the convention for graph datasets by randomly assigning 20 nodes per class for training, 500 for validation, and the remaining for testing. To obtain the best testing performance of baseline models, we conducted a thorough grid search of hyperparameters. We evaluated the accuracy of the validation nodes to identify the best hyperparameters and report the corresponding testing accuracy. Since GNNs are faster to train than convolutional neural networks, we tested all possible combinations of the above parameters for the baseline, conducting 144 searches per model on one dataset. We tested GCN [28], GAT [53], SAGE [24], and APPNP [19] on CoraML, Citeseer, PubMed, Cora and DBLP [7] with detailed tuning. There are only two convolution layers for GNNs, so we only test our algorithm with the scalar prior. We added one dropout layer between two graph convolution layers for baselines only, except keeping the dropout in the attention layers of GAT for both our algorithm and baselines since it is essentially dropping edges of the input graph. In Table 3, for each GNN architecture, the rows of AdamW and scalar, respectively, record the performances of the baseline and the PAC training with early stopping determined by the validation dataset. We see that the results of our algorithm match the best testing accuracy of baselines. We also did a separate experiment by disabling the early stopping and using the training and validation nodes both for training and then we report the performances of the baseline and PAC training. For the baseline, we need to first train the model using only the original training data to detect the best hyperparameters, and then train the model again on the combined data. The rows of AdamW+val

and scalar+val record the performances of the baseline and the PAC training respectively, at full convergences with the combined dataset for training. We can see that testing accuracy after adding validation nodes increased significantly for both methods but still, the results of our algorithm match the best testing accuracy of baselines. We use Adam as the optimizer with the learning rate as  $1e-2$  for all models using both training and validation nodes. Additional training information and evaluation outcomes are in the appendix (Sec. H.3).

**Few-shot text classification with transformers:** The proposed method is also observed to work on transformers network. We conducted experiments on two text classification tasks of the GLUE benchmark as shown in Table 4. We use classification accuracy as the evaluation metric. The baseline method uses grid search over the hyperparameter choices of the learning rate ( $1e-1$ ,  $1e-2$ ,  $1e-3$ ), batch size (2, 8, 16, 32, 80), dropout ratio (0, 0.5), optimization algorithms (SGD, AdamW), noise injection (0,  $1e-5$ ,  $1e-4$ ,  $1e-3$ ,  $1e-2$ ,  $1e-1$ ), and weight decay (0,  $1e-1$ ,  $1e-2$ ,  $1e-3$ ,  $1e-4$ ). The learning rate and batch size of our method are set to  $1e-3$  and 80 (i.e., full-batch), respectively. In this task, the number of training samples is small (80). As a result, the preset  $\gamma_2 = 10$  is a bit large and thus prevents the model from achieving the best performance with PAC-Bayes training. We use the refined procedure described in Sec. H.4<sup>3</sup>.

We adopt BERT [14] as our backbone and added one fully-connect layer to be the classification layer. Only the added classification layer is trainable, and the pre-trained model is frozen without gradient update. To simulate a few-shot learning scenario, we randomly sample 100 instances from the original training set and take the whole development set to evaluate the classification performance. We split the training set into 5 splits, taking one split as the validation data and the rest as the training set. Each experiment was conducted five times, and we report the average performance. We used the PAC-Bayes training with the scalar prior in this experiment. According to Table 4, our method is competitive to the baseline method on the SST task, the performance gap is only 0.4 points. On the QNLI task, our method outperforms the baseline by a large margin, and the variance of our proposed method is less than that of the baseline method. More background about the SST and QNLI tasks are available in the appendix (Sec. H.5)

Table 4: Testing accuracy on the development sets of 2 GLUE benchmarks.

	SST	QNLI
baseline	<b>72.9±0.99</b>	62.6±0.10
scalar	72.5±0.99	<b>64.2±0.02</b>

## 7 Model analysis

We examined the learning process of PAC-Bayes training by analyzing the posterior variance  $\sigma$  for different layers in models trained by Algorithm 3. Typically, batch norm layers have smaller  $\sigma$  values than convolution layers. Additionally, shadow convolution and the last few layers have smaller  $\sigma$  values than the middle layers. We also found that skip-connections in ResNet18 have smaller  $\sigma$  values than nearby layers, suggesting that important layers with a greater impact on the output have smaller  $\sigma$  values.

In Stage 1, the training loss is higher than the testing loss, which means the adopted PAC bound is able to bound the generalization error throughout the PAC training stage. Additionally, we observed that the final value of  $K$  is usually very close to the minimum of the sampled function values. The average value of  $\sigma$  experienced a rapid update during the initial 50 warmup epochs but later progressed slowly until Stage 2. The details can be found in Figure 2. More details are available in the appendix (Sec. H.6).

<sup>3</sup>The refined procedure can be also applied to the CNN and GNN experiments but with smaller improvements than the transformers.

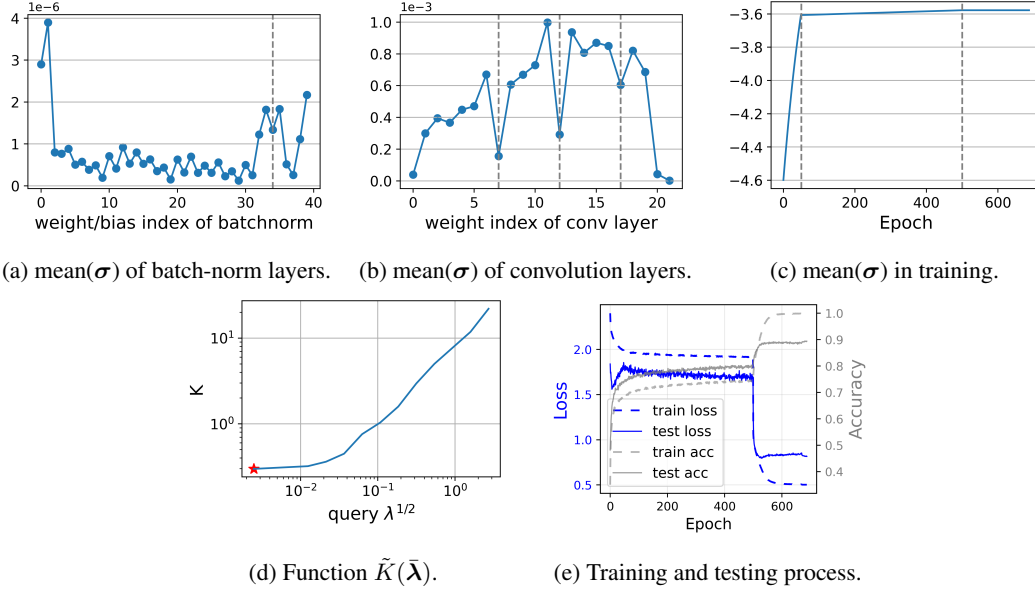


Figure 2: Training details of ResNet18 on CIFAR10. The red star denotes the final  $K$ .

## 8 Limitations of the proposed PAC-Bayes training

In previous sections, we demonstrated the great potential of PAC training. Here we mention some limitations.

1. In conventional training, the weights of the neural network  $\mathbf{h}$  is the only parameter to be stored and updated. In PAC-Bayes training, we have four parameters  $\mathbf{h}, \lambda, \sigma, \gamma$ . Among these variables,  $\gamma$  can be computed on the fly or whenever needed. We need to store  $\mathbf{h}, \lambda, \sigma$ , where  $\sigma$  has the same size as  $\mathbf{h}$  and  $\lambda$  is much smaller. Hence the total storage is approximately doubled. Likewise, we now need to compute the gradient for  $\mathbf{h}, \lambda, \sigma$ , so the cost of automatic differentiation in each iteration is also approximately doubled. In the inference stage, the complexity is the same as in conventional training.
2. The additional parameters to be optimized in PAC-Bayes training inevitably increase the difficulty of the optimization, and the most direct consequence is that there are more parameters to be initialized. In most of the experiments we ran, the recommended initialization of  $\mathbf{v}$  and  $\mathbf{b}$  work well. Rarely is it necessary to modify this setup. But if it occurs (i.e., in some settings, the recommended noise initializations are too large or too small), then the convergence of the algorithm would usually be affected immediately after the training started. So, if one observes a stall in the training accuracy in the early iterations, it usually indicates that the noise initialization requires adjustment, and a simple adjustment of multiplying the noise level by a global scalar often suffices. The tuning of initialization for PAC training (most of the time unnecessary) can be performed much more efficiently than the hyper-parameter tuning for the baseline, as inappropriate noise initializations lead to convergence problems appearing right after the training starts, whereas for the hyperparameter tuning, one needs to wait until the completion of the entire training process to evaluate the effectiveness of the current parameter configuration, which is much more time-consuming.

## 9 Conclusion and future work

In our study, we introduce Auto-tune, a PAC-Bayes method for training deep neural networks, superior to prior methods due to its trainable prior and posterior applicability to over-parameterized networks with unbounded loss, and efficiency without hyper-parameter tuning. It demonstrated competitive performance to grid-search optimized models in experiments with convolutional and graph neural networks. Enhancements to generalization can be achieved through tighter PAC-Bayes bounds. The

learned noise level may be used to defend against gradient inversion attacks and facilitate network quantization.

## Appendix

### A Estimating $K$ in the case of layer-wise prior

When using the layer-wise prior version of our method, the exponential moment bound  $K(\lambda)$  is a  $k$ -dimensional function, and estimating it accurately requires a large number of samples. In this paper, we adopt a simple empirical approach to address this issue. We assume that the original function  $K(\lambda)$  can be well-approximated by a one-dimensional function  $\tilde{K}$  that solely depends on the mean value of the input. That is, we assume there is a one-dimensional function  $\tilde{K}$  such that  $K(\lambda) \approx \tilde{K}(\bar{\lambda})$ , where  $\bar{\lambda}$  denotes the mean of  $\lambda$ . Then we only need to estimate this one-dimensional function  $\tilde{K}$  through function interpolation. We note that one can always choose to directly interpolate the  $k$ -dimensional function  $K(\lambda)$  directly, but at the expense of increased sampling complexity and computational time.

### B Label smoothing

Minimizing the loss and maximizing the accuracy are two separate but related tasks. In the image or node classification task, the goal is to increase the classification accuracy, while in PAC-Bayes training, the goal is to minimize the population loss. However, in cases when accuracy and loss are perfectly negatively correlated, these two goals coincide. With label-smoothing, we observed a larger correlation between the loss and accuracy than without, and therefore we reported results with label-smoothing turned on for both the PAC-Bayes training and the baseline. When the label smoothing is turned off, the performances of the two methods would decrease by comparable amounts.

### C Cautions in choosing $\gamma_2$

Recall that the exponential momentum bound  $K(\lambda)$  is estimated over a range  $[\gamma_1, \gamma_2]$  of  $\gamma$  as per Definition 2. It means that we need the inequality

$$\mathbb{E}_{\mathbf{h} \sim \mathcal{P}_\lambda} \mathbb{E}[\exp(\gamma X(\mathbf{h}))] \leq \exp(\gamma^2 K^2(\lambda))$$

to hold for any  $\gamma$  in this range. One needs to be a little cautious when choosing the upper bound  $\gamma_2$ , because if it is too large, then the empirical version of  $\mathbb{E}_{\mathbf{h} \sim \mathcal{P}} \mathbb{E}[\exp(\gamma X(\mathbf{h}))]$  would be a very poor approximation to the true expectation due to the fact that the variable  $X$  is on the exponent, unless a large amount of samples  $h$  is drawn, which would then be extremely time-consuming and unrealistic in the deep neural network setting. Therefore, we recommended  $\gamma_2$  to be set to 10, or 20 at most, to avoid this issue. Even though in some cases, this means the optimal  $\gamma$  that minimizes the PAC-Bayes bound is ruled out, we found that a more accurate estimation of  $K$  resulting from using the recommended  $\gamma_2$  is more crucial to obtaining the best performance of the PAC-Bayes training. The choice of  $\gamma_1$  is not as critical as the choice of  $\gamma_2$ . But a smaller  $\gamma_1$  usually means a larger value of  $K(\lambda)$  for any given  $\lambda$ , and therefore a looser PAC-Bayes bound and worse performance.

### D Initialization of GNNs

Typically, the training dataset for a graph neural network is quite small. As a result, the KL term in the PAC-Bayes loss gets large easily provided the initialization of the noise is not sufficiently good. This poses a challenge in initializing the PAC-Bayes training process. Although the proposed initialization in Algorithm 2 works well for most GNN networks and datasets, it may fail on some occasions. To address this issue, we modify the initialization by adding a clipping of the noise levels  $\sigma$  and  $\lambda$  at a lower bound of  $-\log(10)$ . For GNN, this operation increases the noise level. Please refer to the paragraph under Remark 5.0.1 for the theoretical reason of the clipping and to Sec. 8 (second item) for how the value  $-\log 10$  is found in practice.

## E Proof of Theorem 4.1

**Theorem E.1.** *Given a prior  $\mathcal{P}_\lambda$  parametrized by  $\lambda \in \Lambda$  over the hypothesis set  $\mathcal{H}$ . Fix  $\lambda \in \Lambda$ ,  $\delta \in (0, 1)$  and  $\gamma \in [\gamma_1, \gamma_2]$ . For any choice of i.i.d  $m$ -sized training dataset  $\mathcal{S}$  according to  $\mathcal{D}$ , and all posterior distributions  $\mathcal{Q}$  over  $\mathcal{H}$ , we have*

$$\mathbb{E}_{\mathbf{h} \sim \mathcal{Q}} \ell(\mathbf{h}; \mathcal{D}) \leq \mathbb{E}_{\mathbf{h} \sim \mathcal{Q}} \ell(\mathbf{h}; \mathcal{S}) + \frac{1}{\gamma m} \left( \ln \frac{1}{\delta} + \text{KL}(\mathcal{Q} \parallel \mathcal{P}_\lambda) \right) + \gamma K^2(\lambda) \quad (11)$$

holds with probability at least  $1 - \delta$  when  $\ell(\mathbf{h}, \cdot)$  satisfies Definition 2 with bound  $K(\lambda)$ .

**Proof.** Firstly, in the bounded interval specified, we bound the difference of the expected loss over the posterior distribution evaluated on the training dataset  $\mathcal{S}$  and  $\mathcal{D}$  with the KL-divergence between the Posterior distribution  $\mathcal{Q}$  and prior distribution  $\mathcal{P}_\lambda$  evaluated over a hypothesis space  $\mathcal{H}$ . For  $\gamma \in [\gamma_1, \gamma_2]$ ,

$$\begin{aligned} & \mathbb{E}_{\mathcal{S} \sim \mathcal{D}} [\exp(\gamma m (\mathbb{E}_{\mathbf{h} \sim \mathcal{Q}} \ell(\mathbf{h}; \mathcal{D}) - \mathbb{E}_{\mathbf{h} \sim \mathcal{Q}} \ell(\mathbf{h}; \mathcal{S})) - \text{KL}(\mathcal{Q} \parallel \mathcal{P}_\lambda))] \\ &= \mathbb{E}_{\mathcal{S} \sim \mathcal{D}} [\exp(\gamma m (\mathbb{E}_{\mathbf{h} \sim \mathcal{Q}} \ell(\mathbf{h}; \mathcal{D}) - \mathbb{E}_{\mathbf{h} \sim \mathcal{Q}} \ell(\mathbf{h}; \mathcal{S})) - \mathbb{E}_{\mathbf{h} \sim \mathcal{Q}} \frac{d\mathcal{Q}}{d\mathcal{P}_\lambda}(\mathbf{h}))] \end{aligned} \quad (12)$$

$$\leq \mathbb{E}_{\mathcal{S} \sim \mathcal{D}} \mathbb{E}_{\mathbf{h} \sim \mathcal{Q}} [\exp((\gamma m (\ell(\mathbf{h}; \mathcal{D}) - \ell(\mathbf{h}; \mathcal{S})) - \log \frac{d\mathcal{Q}}{d\mathcal{P}_\lambda}(\mathbf{h})))] \quad (13)$$

$$\begin{aligned} &= \mathbb{E}_{\mathcal{S} \sim \mathcal{D}} \mathbb{E}_{\mathbf{h} \sim \mathcal{Q}} [\exp(\gamma m (\ell(\mathbf{h}; \mathcal{D}) - \ell(\mathbf{h}; \mathcal{S}))) \frac{d\mathcal{P}_\lambda}{d\mathcal{Q}}(\mathbf{h})] \\ &= \mathbb{E}_{\mathcal{S} \sim \mathcal{D}} \mathbb{E}_{\mathbf{h} \sim \mathcal{P}_\lambda} [\exp(\gamma m (\ell(\mathbf{h}; \mathcal{D}) - \ell(\mathbf{h}; \mathcal{S}))) \frac{d\mathcal{P}_\lambda}{d\mathcal{Q}}(\mathbf{h}) \frac{d\mathcal{Q}}{d\mathcal{P}_\lambda}(\mathbf{h})] \end{aligned} \quad (14)$$

$$= \mathbb{E}_{\mathbf{h} \sim \mathcal{P}_\lambda} \mathbb{E}_{\mathcal{S} \sim \mathcal{D}} [\exp(\gamma m (\ell(\mathbf{h}; \mathcal{D}) - \ell(\mathbf{h}; \mathcal{S}))) \frac{d\mathcal{Q}}{d\mathcal{P}_\lambda}(\mathbf{h})] \quad (15)$$

where  $d\mathcal{Q}/d\mathcal{P}$  denotes the Radon-Nikodym derivative. In 12, we use  $\text{KL}(\mathcal{Q} \parallel \mathcal{P}_\lambda) = \mathbb{E}_{\mathbf{h} \sim \mathcal{Q}} \frac{d\mathcal{Q}}{d\mathcal{P}_\lambda}(\mathbf{h})$ . From 12 to 13, Jensen's inequality is used over the convex exponential function. And in 14, the expectation is changed to the prior distribution from the posterior.

Let  $X = \ell(\mathbf{h}; \mathcal{D}) - \ell(\mathbf{h}; \mathcal{S})$ , then  $X$  is centered with  $\mathbb{E}[X] = 0$ . Then, by Definition 1,

$$\exists \mathbb{E}_{\mathbf{h} \sim \mathcal{P}_\lambda} \mathbb{E}_{\mathcal{S} \sim \mathcal{D}} [\exp(\gamma m X)] \leq \exp(m\gamma^2 K^2(\lambda)). \quad (16)$$

Using Markov's inequality, (17) holds with probability at least  $1 - \delta$ .

$$\exp(\gamma m X) \leq \frac{\exp(m\gamma^2 K^2(\lambda))}{\delta}. \quad (17)$$

Combining (15) and (17), the following inequality holds with probability at least  $1 - \delta$ .

$$\begin{aligned} & \exp(\gamma m (\mathbb{E}_{\mathbf{h} \sim \mathcal{Q}} \ell(\mathbf{h}; \mathcal{D}) - \mathbb{E}_{\mathbf{h} \sim \mathcal{Q}} \ell(\mathbf{h}; \mathcal{S})) - \text{KL}(\mathcal{Q} \parallel \mathcal{P}_\lambda)) \leq \frac{\exp(m\gamma^2 K^2(\lambda))}{\delta} \\ & \Rightarrow \gamma m (\mathbb{E}_{\mathbf{h} \sim \mathcal{Q}} \ell(\mathbf{h}; \mathcal{D}) - \mathbb{E}_{\mathbf{h} \sim \mathcal{Q}} \ell(\mathbf{h}; \mathcal{S})) - \text{KL}(\mathcal{Q} \parallel \mathcal{P}_\lambda) \leq \ln \frac{1}{\delta} + m\gamma^2 K^2(\lambda) \\ & \Rightarrow \mathbb{E}_{\mathbf{h} \sim \mathcal{Q}} \ell(\mathbf{h}; \mathcal{D}) \leq \mathbb{E}_{\mathbf{h} \sim \mathcal{Q}} \ell(\mathbf{h}; \mathcal{S}) + \frac{1}{\gamma m} \left( \ln \frac{1}{\delta} + \text{KL}(\mathcal{Q} \parallel \mathcal{P}_\lambda) \right) + \gamma K^2(\lambda) \end{aligned} \quad (18)$$

The bound 18 is exactly the statement of the Theorem. □

## F Proof of Theorem 4.2

**Theorem F.1.** *Let  $n(\epsilon) := \mathcal{N}(\Lambda, \|\cdot\|, \epsilon)$  be the covering number of the set of the prior parameters  $\Lambda$ . Under Assumption 4.1.1 and Assumption 4.1.2, the following inequality holds for the minimizer  $(\hat{\mathbf{h}}, \hat{\gamma}, \hat{\sigma}, \hat{\lambda})$  of upper bound in 4 with probability at least  $1 - \epsilon$ :*

$$\begin{aligned} \mathbb{E}_{\mathbf{h} \sim \mathcal{Q}_{\hat{\sigma}}(\hat{\mathbf{h}})} \ell(\mathbf{h}; \mathcal{D}) &\leq \mathbb{E}_{\mathbf{h} \sim \mathcal{Q}_{\hat{\sigma}}(\hat{\mathbf{h}})} \ell(\mathbf{h}; \mathcal{S}) + \frac{1}{\hat{\gamma} m} \left[ \ln \frac{n(\epsilon)}{\epsilon} + \text{KL}(\mathcal{Q}_{\hat{\sigma}}(\hat{\mathbf{h}}) \parallel \mathcal{P}_{\hat{\lambda}}) \right] + \hat{\gamma} K^2(\hat{\lambda}) + \eta \\ &= L_{PAC}(\hat{\mathbf{h}}, \hat{\gamma}, \hat{\sigma}, \hat{\lambda}) + \eta + \frac{\ln(n(\epsilon))}{\hat{\gamma} m} \end{aligned} \quad (19)$$

holds for any  $\epsilon, \varepsilon > 0$ , where  $\eta = (\frac{1}{\gamma_1 m} + \gamma_2)(\eta_1(\varepsilon) + \eta_2(\varepsilon))$ .

**Proof:** In this proof, we extend the data-independent PAC-Bayes bound of 4 to the data-dependent one that accommodates the error when the prior distribution  $\mathfrak{P} = \{P_{\lambda}, \lambda \in \Lambda \subseteq \mathbb{R}^k\}$  is parameterized by and optimized over a finite set of parameters with a much smaller dimension than the model itself. Let  $\mathbb{T}(\Lambda, \|\cdot\|, \varepsilon)$  be an  $\varepsilon$ -cover of the set  $\Lambda$ , which states that for any  $\lambda \in \Lambda$ , there exists a  $\tilde{\lambda} \in \mathbb{T}(\Lambda, \|\cdot\|, \varepsilon)$ , such that  $\|\lambda - \tilde{\lambda}\| \leq \varepsilon$ . Assumption 4.1.1 and Assumption 4.1.2.

Now we select the posterior distribution as  $\mathcal{Q}_{\sigma}(\mathbf{h}) := \mathbf{h} + \mathcal{Q}_{\sigma}$ , where  $\mathbf{h}$  is the current model and  $\mathcal{Q}_{\sigma}$  is a zero mean distribution parameterized by  $\sigma \in \mathbb{R}^d$ . Assuming the prior  $\mathcal{P}$  is parameterized by  $\lambda \in \mathbb{R}^k$  ( $k \ll m, d$ ).

Then the PAC-Bayes bound in 4 holds already for any  $(\hat{\mathbf{h}}, \hat{\gamma}, \hat{\sigma}, \lambda), \lambda \in \Lambda$ , i.e.,

$$\mathbb{E}_{\tilde{\mathbf{h}} \sim \mathcal{Q}_{\hat{\sigma}}(\hat{\mathbf{h}})} \ell(\tilde{\mathbf{h}}; \mathcal{D}) \leq \mathbb{E}_{\tilde{\mathbf{h}} \sim \mathcal{Q}_{\hat{\sigma}}(\hat{\mathbf{h}})} \ell(\tilde{\mathbf{h}}; \mathcal{S}) + \frac{1}{\hat{\gamma}m} (\ln \frac{1}{\delta} + \text{KL}(\mathcal{Q}_{\hat{\sigma}}(\hat{\mathbf{h}}) \parallel \mathcal{P}_{\lambda})) + \hat{\gamma} K^2(\lambda) \quad (20)$$

with probability over  $1 - \delta$ .

Now, for the collection of  $\lambda$ s in the  $\varepsilon$ -net  $\mathbb{T}(\Lambda, \|\cdot\|, \varepsilon)$ , by the union bound, the PAC-Bayes bound uniformly holds with probability at least  $1 - |\mathbb{T}|\delta = 1 - n\delta$ . Now for an arbitrary  $\lambda \in \Lambda$ , its distance to the  $\varepsilon$ -net is at most  $\varepsilon$ . Then under Assumption 4.1.1 and Assumption 4.1.2, we have:

$$\min_{\tilde{\lambda} \in \mathbb{T}} |\text{KL}(\mathcal{Q} \parallel \mathcal{P}_{\lambda}) - \text{KL}(\mathcal{Q} \parallel \mathcal{P}_{\tilde{\lambda}})| \leq \eta_1(\|\lambda - \tilde{\lambda}\|) \leq \eta_1(\varepsilon),$$

and

$$\min_{\tilde{\lambda} \in \mathbb{T}} |K^2(\lambda) - K^2(\tilde{\lambda})| \leq \eta_2(\|\lambda - \tilde{\lambda}\|) \leq \eta_2(\varepsilon).$$

With these two inequalities, we can control the PAC-Bayes loss at the given  $\lambda$  as follows:

$$\min_{\tilde{\lambda} \in \mathbb{T}} |L_{PAC}(\hat{\mathbf{h}}, \hat{\gamma}, \hat{\sigma}, \lambda) - L_{PAC}(\hat{\mathbf{h}}, \hat{\gamma}, \hat{\sigma}, \tilde{\lambda})| \leq \frac{1}{\hat{\gamma}m} \eta_1(\varepsilon) + \hat{\gamma} \eta_2(\varepsilon) \leq \frac{1}{\gamma_1 m} \eta_1(\varepsilon) + \gamma_2 \eta_2(\varepsilon) \leq C(\eta_1(\varepsilon) + \eta_2(\varepsilon))$$

where  $C = \frac{1}{\gamma_1 m} + \gamma_2$  and  $\gamma \in [\gamma_1, \gamma_2]$ . Now, since this inequality holds for any  $\lambda \in \Lambda$ , it certainly holds for the optima  $\hat{\lambda}$ . Combining this with (20), we have

$$\mathbb{E}_{\tilde{\mathbf{h}} \sim \mathcal{Q}_{\hat{\sigma}}(\hat{\mathbf{h}})} \ell(\tilde{\mathbf{h}}; \mathcal{D}) \leq L_{PAC}(\hat{\mathbf{h}}, \hat{\gamma}, \hat{\sigma}, \hat{\lambda}) + C(\eta_1(\varepsilon) + \eta_2(\varepsilon))$$

where  $C := \frac{1}{\gamma_1 m} + \gamma_2$ .

Now taking  $\epsilon := n\delta$ , we get, with probability  $1 - \epsilon$ , it holds that

$$\mathbb{E}_{\tilde{\mathbf{h}} \sim \mathcal{Q}_{\hat{\sigma}}(\hat{\mathbf{h}})} \ell(\tilde{\mathbf{h}}; \mathcal{D}) \leq \mathbb{E}_{\tilde{\mathbf{h}} \sim \mathcal{Q}_{\hat{\sigma}}(\hat{\mathbf{h}})} \ell(\tilde{\mathbf{h}}; \mathcal{S}) + \frac{1}{\hat{\gamma}m} (\ln \frac{n(\varepsilon)}{\epsilon} + \text{KL}(\mathcal{Q}_{\hat{\sigma}}(\hat{\mathbf{h}}) \parallel \mathcal{P}_{\hat{\lambda}})) + \hat{\gamma} K^2(\hat{\lambda}) + C(\eta_1(\varepsilon) + \eta_2(\varepsilon))$$

and the proof is completed.  $\square$

## G Proof of Corollary 5.0.1

Recall for the training, we proposed to optimize over all four variables  $\mathbf{h}$ ,  $\gamma$ ,  $\sigma$ , and  $\lambda$ .

$$(\hat{\mathbf{h}}, \hat{\gamma}, \hat{\sigma}, \hat{\lambda}) = \arg \min_{\substack{\mathbf{h}, \lambda, \sigma, \\ \gamma \in [\gamma_1, \gamma_2]}} \underbrace{\mathbb{E}_{\tilde{\mathbf{h}} \sim \mathcal{Q}_{\sigma}(\mathbf{h})} \ell(\tilde{\mathbf{h}}; \mathcal{S}) + \frac{1}{\gamma m} (\ln \frac{1}{\delta} + \text{KL}(\mathcal{Q}_{\sigma}(\mathbf{h}) \parallel \mathcal{P}_{\lambda})) + \gamma K^2(\lambda)}_{\equiv L_{PAC}(\mathbf{h}, \gamma, \sigma, \lambda)}. \quad (21)$$

**Corollary G.0.1.** Assume the parameter sets of priors and posteriors are both bounded,  $\mathcal{H} := \{\mathbf{h} \in \mathbb{R}^d : \|\mathbf{h}\|_2 \leq M\}$ ,  $\Sigma := \{\sigma \in \mathbb{R}_+^d : \|\sigma\|_1 \leq T\}$ ,  $\Lambda := \{\lambda \in [e^{-a}, e^b]^k\}$ , and assume  $\ell(\mathbf{h}, \cdot)$  satisfies Definition 2 with bound  $K(\lambda)$  and  $K^2(\lambda)$  is Lipschitz continuous with Lipschitz constant  $C_K$ . Then with high probability, the PAC-Bayes bound for the minimizer of (P) has the form

$$\mathbb{E}_{\tilde{\mathbf{h}} \sim \mathcal{Q}_{\hat{\sigma}}(\hat{\mathbf{h}})} \ell(\tilde{\mathbf{h}}; \mathcal{D}) \leq L_{PAC}(\hat{\mathbf{h}}, \hat{\gamma}, \hat{\sigma}, \hat{\lambda}) + \eta,$$

where  $\eta = \frac{k}{\gamma_1 m} \left(1 + \ln \frac{C(C_K + L(d))(b+a)\gamma_1 m}{2k}\right)$ ,  $C = \frac{1}{\gamma_1 m} + \gamma_2$ ,  $L(d) = \frac{1}{2} \max\{d, e^a(2M + T)\}$

**Proof:** The above Corollary is an extension of the previous theorem, with a more explicit expression when the bounds for the hypothesis parameter  $\mathbf{h}$ , prior variance parameter  $\boldsymbol{\lambda}$  and posterior variance parameter  $\boldsymbol{\sigma}$  are known.

For a  $k$ -layer network, the prior is written as  $\mathcal{P}_{\boldsymbol{\lambda}}(\mathbf{h}_0)$ , where  $\boldsymbol{\lambda} \in \mathbb{R}_+^k$  is the vector containing the variance for each layer. The set of all such priors is denoted by  $\mathfrak{P} := \{\mathcal{P}_{\boldsymbol{\lambda}}(\mathbf{h}_0), \boldsymbol{\lambda} \in \Lambda\}$ . We select the posterior distribution to be centered around the trained model  $\mathbf{h}$ , with independent anscalar variance. Specifically, for a network with  $d$  trainable parameters, the posterior is set to  $\mathcal{Q}_{\boldsymbol{\sigma}}(\mathbf{h}) := \mathcal{N}(\mathbf{h}, \text{diag}(\boldsymbol{\sigma}))$ , where  $\mathbf{h}$  is the mean and  $\boldsymbol{\sigma} \in \mathbb{R}_+^d$  is the vector containing the variance for each trainable parameter. The set of all posteriors is  $\mathfrak{Q} := \{\mathcal{Q}_{\boldsymbol{\sigma}}(\mathbf{h}), \boldsymbol{\sigma} \in \Sigma, \mathbf{h} \in \mathcal{H}\}$ , and the KL divergence between such prior and posterior is

$$\text{KL}(\mathcal{Q}_{\boldsymbol{\sigma}}(\mathbf{h}) \parallel \mathcal{P}_{\boldsymbol{\lambda}}(\mathbf{h}_0)) = \frac{1}{2} \sum_{i=1}^k \left[ -\mathbf{1}_{d_i}^\top \ln(\boldsymbol{\sigma}_i) + d_i(\ln(\lambda_i) - 1) + \frac{1}{\lambda_i}(\|\boldsymbol{\sigma}_i\|_1 + \|(\mathbf{h} - \mathbf{h}_0)_i\|^2) \right], \quad (22)$$

where  $\boldsymbol{\sigma}_i, (\mathbf{h} - \mathbf{h}_0)_i$  are vectors denoting the variances and weights for the  $i$ -th layer, respectively, and  $\lambda_i$  is the scalar variance for the  $i$ -th layer.  $d_i = \dim(\boldsymbol{\sigma}_i)$ , and  $\mathbf{1}_{d_i}$  denotes an all-ones vector of length  $d_i$ .

Letting  $v_i = \log 1/\lambda_i$ ,  $i = 1, \dots, k$  and doing a change of variable  $\tilde{\mathcal{P}}_{\mathbf{v}} := \mathcal{P}_{\boldsymbol{\lambda}} = \mathcal{N}(0, [\text{diag}(\lambda_i I_{d_i})]) = \mathcal{N}(0, [\text{diag}(e^{-v_i} I_{d_i})])$ , where  $d_i$  is the number of trainable parameters in the  $i$ th layer.

$$\frac{\partial \text{KL}(\mathcal{Q}_{\boldsymbol{\sigma}} \parallel \tilde{\mathcal{P}}_{\mathbf{v}})}{\partial v_i} = \frac{1}{2} [-d_i + e^{v_i}(\|\boldsymbol{\sigma}_i\|_1 + \|\mathbf{h}_i - \mathbf{h}_{0,i}\|^2)],$$

where  $\boldsymbol{\sigma}_i, \mathbf{h}_i, \mathbf{h}_{0,i}$  are the blocks of  $\boldsymbol{\sigma}, \mathbf{h}, \mathbf{h}_0$ , corresponding to the  $i$ th layer, respectively. Now, given the assumptions on the bounds in the statement of the corollary, we have:

$$\|\nabla_{\mathbf{v}} \text{KL}(\mathcal{Q}_{\boldsymbol{\sigma}} \parallel \tilde{\mathcal{P}}_{\mathbf{v}})\|_2 \leq \|\nabla_{\mathbf{v}} \text{KL}(\mathcal{Q}_{\boldsymbol{\sigma}} \parallel \tilde{\mathcal{P}}_{\mathbf{v}})\|_1 \leq \frac{1}{2} \max\{d, e^a(2M + T)\} \equiv L(d) \quad (23)$$

where we used the assumption  $\|\boldsymbol{\sigma}\|_1 \leq T$  and  $\|\mathbf{h}_0\|, \|\mathbf{h}\| \leq M$

(23) says  $L(d)$  is a valid Lipschitz bound on the KL divergence and therefore Assumption 4.1.1 is satisfied by setting  $\eta_1(x) = L(d)x$ .

Then we can apply Theorem 4.2, to get with probability  $1 - \epsilon$ ,

$$\mathbb{E}_{\mathbf{h} \sim \mathcal{Q}_{\hat{\boldsymbol{\sigma}}}(\hat{\mathbf{h}})} \ell(\mathbf{h}; \mathcal{D}) \leq \mathbb{E}_{\mathbf{h} \sim \mathcal{Q}_{\hat{\boldsymbol{\sigma}}}(\hat{\mathbf{h}})} \ell(\mathbf{h}; \mathcal{S}) + \frac{1}{\hat{\gamma}m} \left[ \ln \frac{n}{\epsilon} + \text{KL}(\mathcal{Q}_{\hat{\boldsymbol{\sigma}}}(\hat{\mathbf{h}}) \parallel \mathcal{P}_{\boldsymbol{\lambda}}) \right] + \hat{\gamma}K^2(\hat{\boldsymbol{\lambda}}) + C(C_K + L(d))\epsilon. \quad (24)$$

Here, we used  $\eta_1(x) = L(d)x$  and  $\eta_2(x) = C_K x$ . Note that for the set  $[-b, a]^k$ , the covering number  $n = \mathcal{N}([-b, a]^k, \|\cdot\|, \epsilon)$  is  $\left(\frac{b+a}{2\epsilon}\right)^k$ . Introducing a new variable  $\rho > 0$ , letting  $\epsilon = \frac{\rho}{C(C_K + L(d))}$  and inserting them to the above, we obtain with probability  $1 - \epsilon$

$$\begin{aligned} & \mathbb{E}_{\mathbf{h} \sim \mathcal{Q}_{\hat{\boldsymbol{\sigma}}}(\hat{\mathbf{h}})} \ell(\mathbf{h}; \mathcal{D}) \\ & \leq \mathbb{E}_{\mathbf{h} \sim \mathcal{Q}_{\hat{\boldsymbol{\sigma}}}(\hat{\mathbf{h}})} \ell(\mathbf{h}; \mathcal{S}) + \frac{1}{\hat{\gamma}m} \left[ \ln \frac{1}{\epsilon} + \text{KL}(\mathcal{Q}_{\hat{\boldsymbol{\sigma}}}(\hat{\mathbf{h}}) \parallel \mathcal{P}_{\boldsymbol{\lambda}}) \right] \\ & \quad + \hat{\gamma}K^2(\hat{\boldsymbol{\lambda}}) + \rho + \frac{k}{\gamma_1 m} \ln \frac{C(C_K + L(d))(b+a)}{2\rho}. \end{aligned}$$

Further making the upper bound tighter by optimizing over  $\rho$ , we obtain

$$\begin{aligned} & \mathbb{E}_{\mathbf{h} \sim \mathcal{Q}_{\hat{\boldsymbol{\sigma}}}(\hat{\mathbf{h}})} \ell(\mathbf{h}; \mathcal{D}) \\ & \leq \mathbb{E}_{\mathbf{h} \sim \mathcal{Q}_{\hat{\boldsymbol{\sigma}}}(\hat{\mathbf{h}})} \ell(\mathbf{h}; \mathcal{S}) + \frac{1}{\hat{\gamma}m} \left[ \ln \frac{1}{\epsilon} + \text{KL}(\mathcal{Q}_{\hat{\boldsymbol{\sigma}}}(\hat{\mathbf{h}}) \parallel \mathcal{P}_{\boldsymbol{\lambda}}) \right] \\ & \quad + \hat{\gamma}K^2(\hat{\boldsymbol{\lambda}}) + \frac{k}{\gamma_1 m} \left( 1 + \ln \frac{C(C_K + L(d))(b+a)\gamma_1 m}{2k} \right). \end{aligned}$$

□

Table 5: Testing accuracy of ResNet18 trained with different learning rates.

lr	$3e-5$	$5e-5$	$1e-4$	$2e-4$	$3e-4$	$5e-4$
CIFAR10	88.4	88.8	89.3	88.6	88.3	89.2
CIFAR100	69.2	69.0	68.9	69.1	69.1	69.6

## H More Experiment details

We conducted experiments using eight A5000 GPUs that were powered by four AMD EPYC 7543 32-Core Processors. To speed up the training process for posterior and prior variance, we utilized a warmup method that involved updating the noise level in the posterior of each layer as a scalar for the first 50 epochs and then proceeding with normal updates after the warmup period. This method only affects the convergence speed, not the generalization, and it was only used for large models in image classification.

### H.1 Image classification

There is no data augmentation in our experiments. The implementation is based on the GitHub repo [1]. For the layer-wised prior, we treated each parameter in the PyTorch object `model.parameters()` as an independent layer, i.e., the weights and bias of one convolution/batch-norm layer were treated as two different layers. The number of training epochs of Stage 1 is 500 epochs for PAC-Bayes training. Moreover, a learning rate scheduler was added to both our method and the baseline to make the training fully converge. Specifically, the learning rate will be reduced by 0.1 whenever the training accuracy did not increase for 20 epochs. For PAC-Bayes training, the scheduler is only activated in Stage 2. The training will be terminated when the training accuracy is above 99.9% for 20 epochs, or when the learning rate decreased to below  $1e-5$ . We also add label smoothing (0.1) [51] to all models, as discussed in Sec. B.

The testing accuracy from all experiments with batch size 128 with the learning rate  $1e-4$  is shown in Figure 3 and Figure 4. We also visualize the sorted testing accuracy of baselines and our proposed PAC-Bayes training with large batch sizes and a larger learning rate  $5e-4$  (used only to obtain faster convergence) in Figure 5 and Figure 6. These figures demonstrate that our PAC-Bayes training algorithm achieves better testing accuracy than most searched settings. For models VGG13 and ResNet18, the large batch size is 2048, and for large models VGG19 and ResNet34, the large batch size is set to 1280 due to the GPU memory limitation.

### H.2 Ablation study

We conducted an ablation study to showcase some extra benefits of the proposed PAC-Bayes training algorithm besides its ability to achieve auto-tuning. Specifically, we tested the effect of different learning rates on ResNet18 and VGG13 models trained with layer-wise prior. Learning rate has long been known as an important impact factor of the generalization for baseline training. Within the stability range of gradient descent, the larger the learning rate is, the better the generalization has been observed [35]. In contrast, the generalization of the PAC-Bayes trained model is less sensitive to the learning rate. We do observe that due to the newly introduced noise parameters, the stability of the optimization gets worse, which in turn requires a smaller learning rate to achieve stable training. But as long as the stability is guaranteed by setting the learning rate small enough, our results, as Table 5 and 6, indicated that the testing accuracy remained stable across various learning rates for VGG13 and Resnet18. The dash in the table means that the learning rate for that particular setting might be too large to main the stability of the algorithm. For learning rates below  $1e-4$ , we trained the model in Stage 1 for more epochs (700) to fully update the prior and posterior variance.

We also demonstrate that the warmup iterations (as discussed at the beginning of this section) do not affect generalization. As shown in Table 7, the testing accuracy is insensitive to different numbers of warmup iterations.

Table 6: Testing accuracy of VGG13 trained with different learning rates.

lr	$3e-5$	$5e-5$	$1e-4$	$2e-4$	$3e-4$	$5e-4$
CIFAR10	88.6	88.9	89.7	89.6	89.6	89.5
CIFAR100	67.7	68.0	67.1	-	-	-

Table 7: Testing accuracy of ResNet18 trained with warmup epochs of  $\sigma$ .

	10	20	50	80	100	150
CIFAR10	88.5	88.5	89.3	89.5	89.5	88.9
CIFAR100	69.4	69.6	68.9	69.1	69.0	68.1

### H.3 Node classification

We test the PAC-Bayes training algorithm on the following popular GNN models .

- GCN [28]: the number of filters is 32.
- SAGE [24]: the number of filters is 32.
- GAT [53]: the number of filters is 8, the number of heads is 8, and the dropout rate of the attention coefficient is 0.6.
- APPNP [19]: the number of filters is 32,  $K = 10$  and  $\alpha = 0.1$ .

We set the number of layers to 2, which achieves the best performance for the baseline. A ReLU activation and a dropout layer are added in between the two convolution layers. All search details are visualized in Figure 7-10. Our proposed PAC-Bayes training with the scalar prior is better than most of the settings during searching and achieved comparable testing accuracy when adding validation nodes to training.

### H.4 Further improvement of the PAC-training through refining the range of $\gamma$

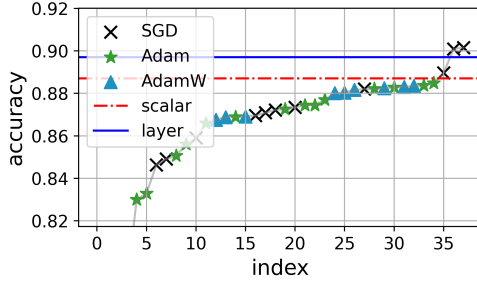
As per Definition 1, the function  $K$  depends on the range  $[\gamma_1, \gamma_2]$  of  $\gamma$ . The preset values of  $\gamma_1$  and  $\gamma_2$  may not be optimal for a given dataset. If the predefined range is too large, then it may result in a large  $K$  and then a vacuous PAC bound. If the range is too small, then it may not contain the optimal  $\gamma$  that minimizes the PAC loss and again result in a vacuous PAC bound. To resolve this issue, we recommend estimating the range of  $\gamma$  using a few iterations and then use the estimated range to do the PAC training. Specifically, we use the preset  $\gamma_1$  and  $\gamma_2$  to train the network for a certain number of epochs and compute the  $\gamma^*$  as according to equation (9). Afterward, we reset the model to its initial weights and noise levels and optimize  $L_{PAC}$  with  $\gamma_1, \gamma_2$  both set to the optimal  $\gamma^*$ .

### H.5 Datasets of few-shot text classification

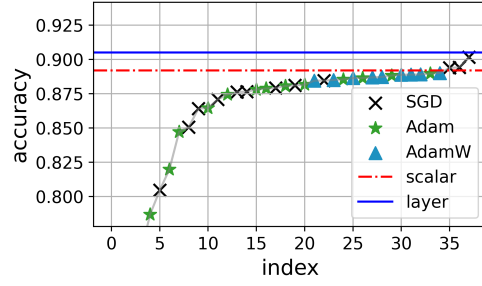
SST is the sentiment analysis task, whose performance is evaluated as the classification accuracy. Sentiment analysis is the process of analyzing the sentiment of a given text to determine if the emotional tone of the text is positive, negative, or neutral. QNLI (Question-answering Natural Language Inference) focuses on determining the logical relationship between a given question and a corresponding sentence. The objective of QNLI is to determine whether the sentence contradicts, entails, or is neutral with respect to the question.

### H.6 Model analysis

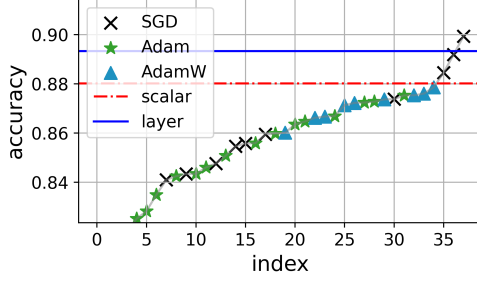
We analyzed models ResNet18, ResNet34 and VGG13 on CIFAR10 and CIFAR100. The details can be found in Figure 11-15. Based on the figures, shadow convolution and the last few layers have smaller  $\sigma$  values than the middle layers for all models. We also found that skip-connections in ResNet18 and ResNet34 have smaller  $\sigma$  values than nearby layers on both datasets, suggesting that important layers with a greater impact on the output have smaller  $\sigma$  values.



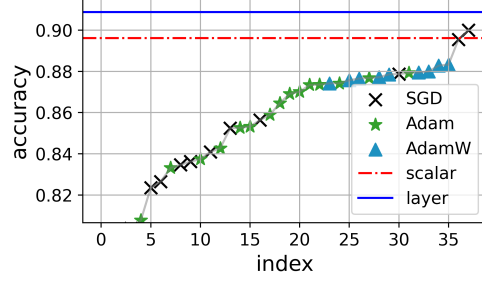
(a) VGG13



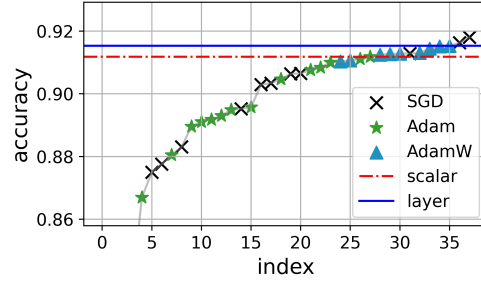
(b) VGG19



(c) ResNet18



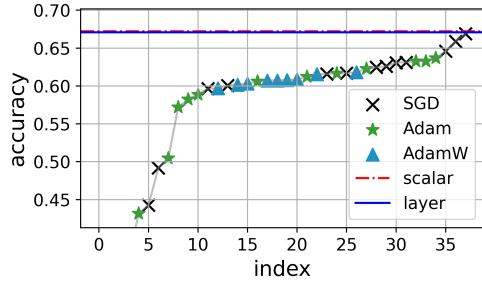
(d) ResNet34



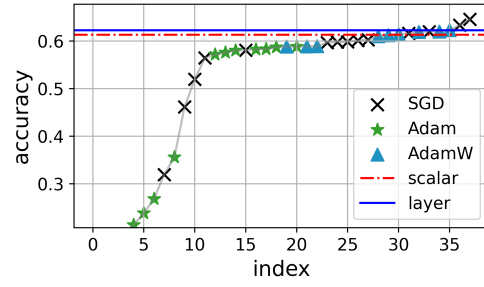
(e) Desnse121

Figure 3: Sorted testing accuracy of CIFAR10. The x-axis represents the experiment index.

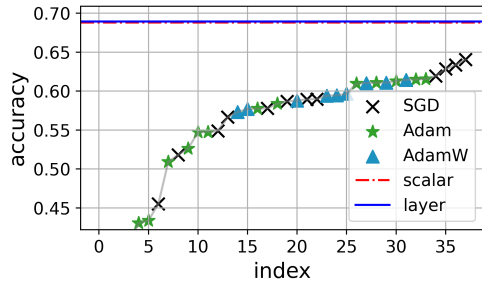
In Stage 1, the training loss is higher than the testing loss, which means the adopted PAC-Bayes bound is able to bound the generalization error throughout the PAC training stage. Moreover, the final value of  $K$  is usually very close to the minimum of the sampled function values. The average value of  $\sigma$  experienced a rapid update during the initial 50 warmup epochs but later progressed slowly until Stage 2.



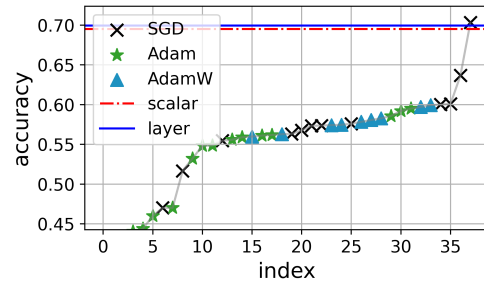
(a) VGG13



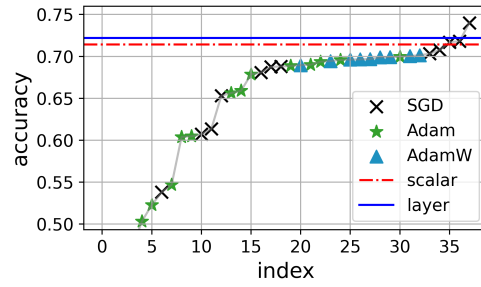
(b) VGG19



(c) ResNet18

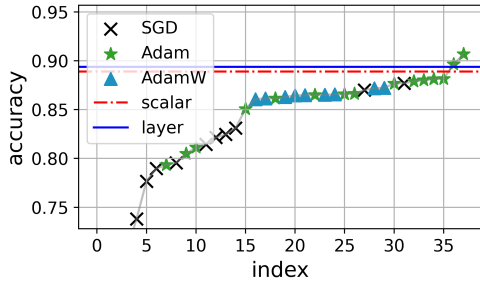


(d) ResNet34

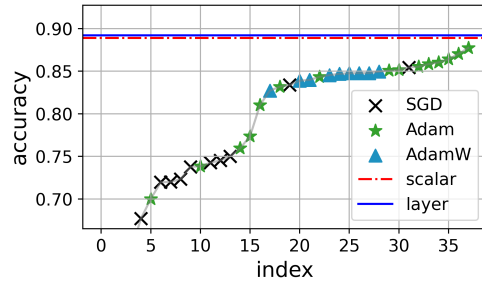


(e) Desnse121

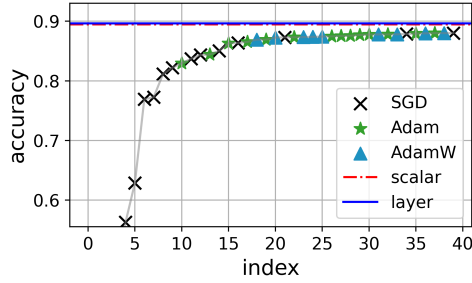
Figure 4: Sorted testing accuracy of CIFAR100. The x-axis represents the experiment index.



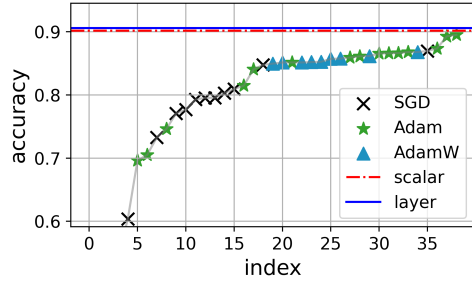
(a) VGG13 (batch: 2048)



(b) ResNet18 (batch: 2048)

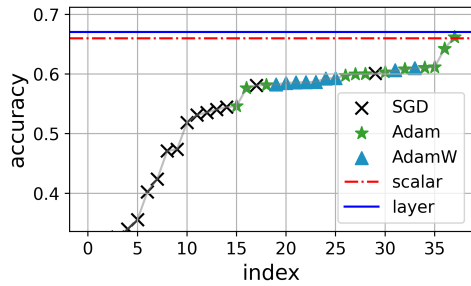


(c) VGG19 (batch: 1280)

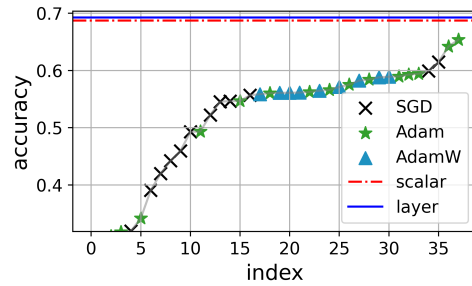


(d) ResNet34 (batch: 1280)

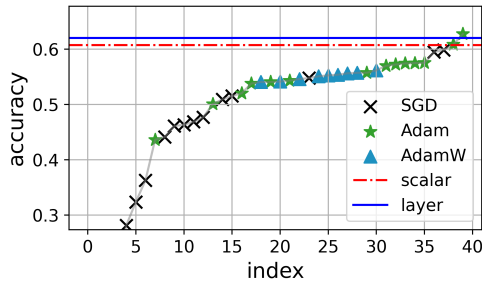
Figure 5: Sorted testing accuracy of CIFAR10 with large batch sizes. The x-axis represents the experiment index.



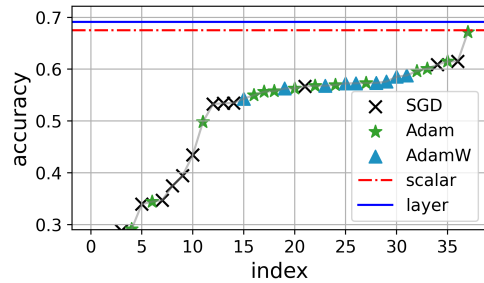
(a) VGG13 (batch: 2048)



(b) ResNet18 (batch: 2048)



(c) VGG19 (batch: 1280)



(d) ResNet34 (batch: 1280)

Figure 6: Sorted testing accuracy of CIFAR100 with large batch sizes. The x-axis represents the experiment index.

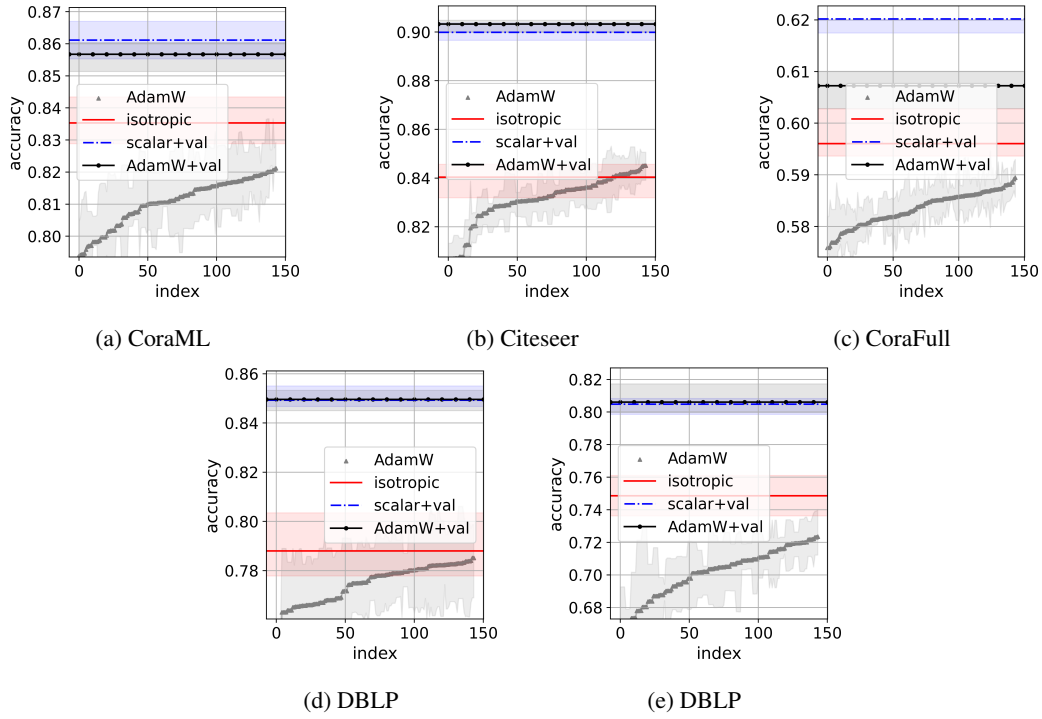


Figure 7: Testing accuracy of GCN. The interval is constructed by the first and third quartiles over the ten random splits.

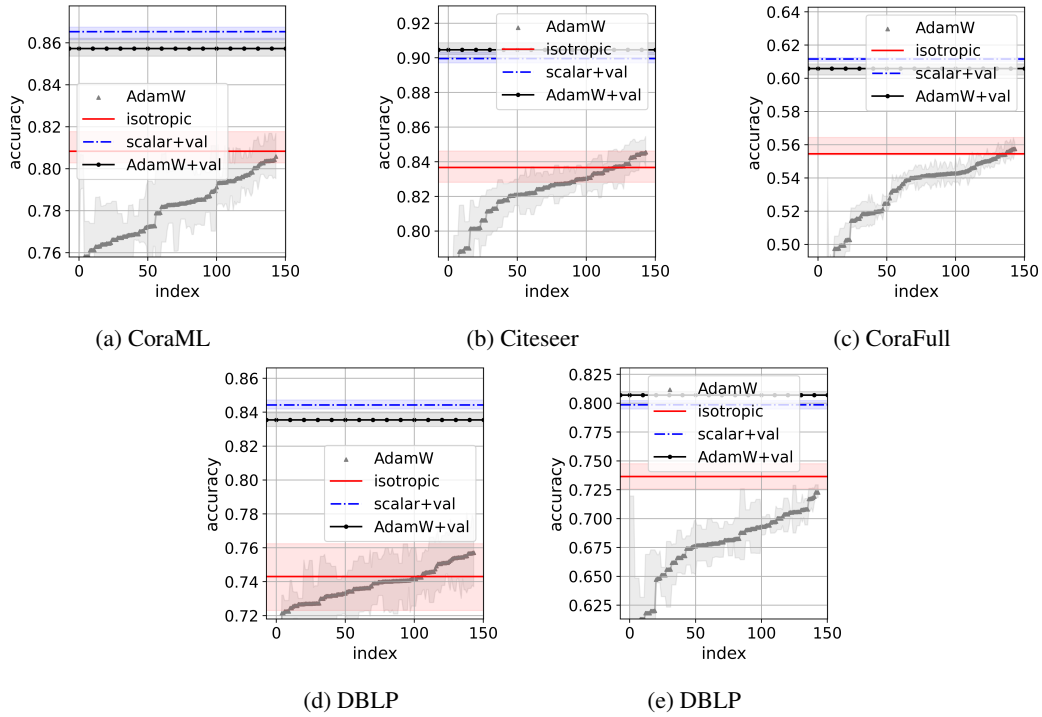


Figure 8: Testing accuracy of SAGE. The interval is constructed by the first and third quartiles over the ten random splits.

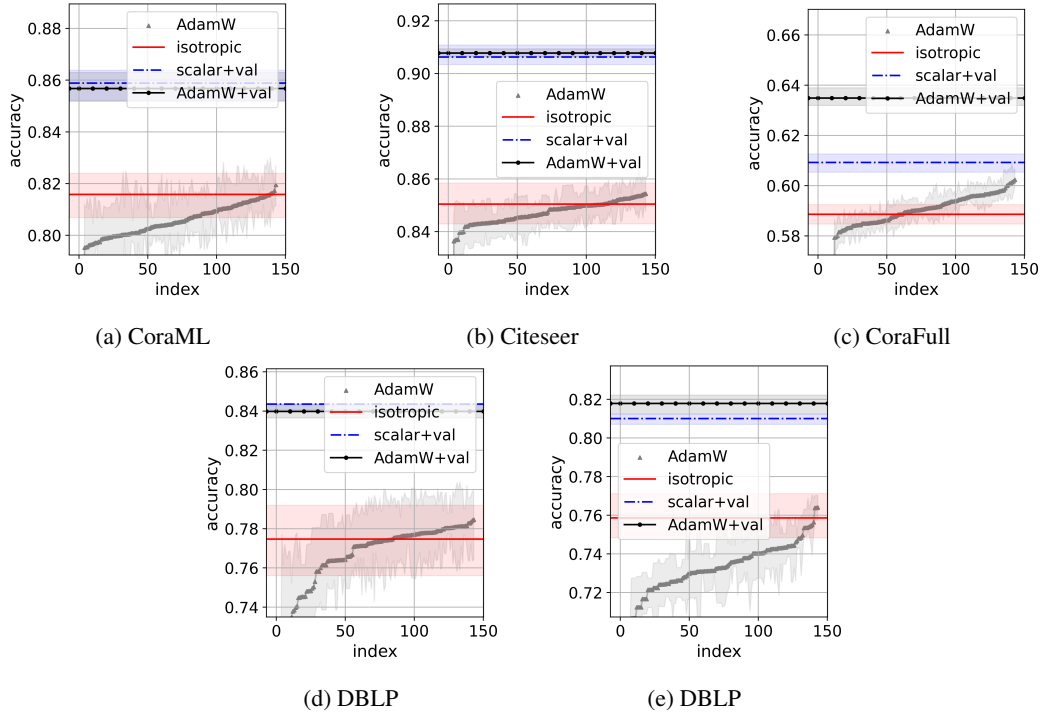


Figure 9: Testing accuracy of GAT. The interval is constructed by the first and third quartiles over the ten random splits.

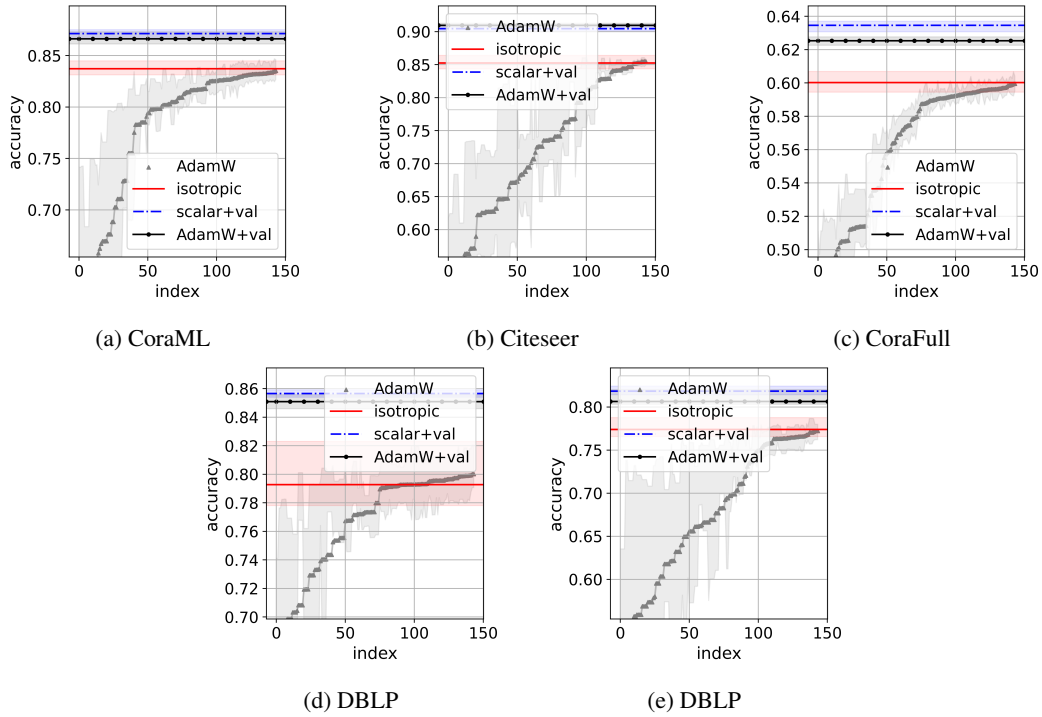


Figure 10: Testing accuracy of APPNP. The interval is constructed by the first and third quartiles over the ten random splits.

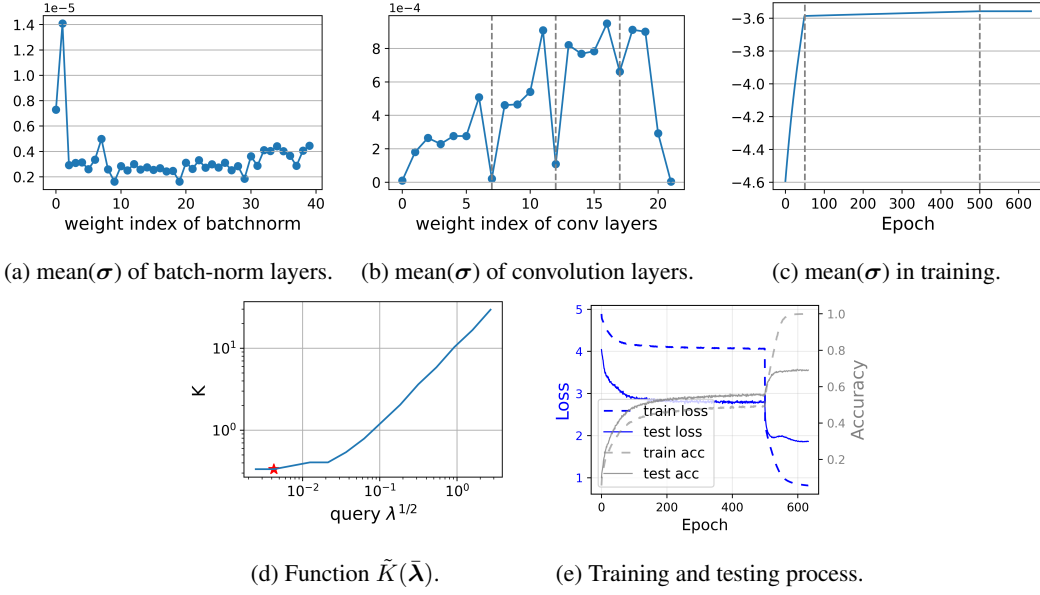


Figure 11: Training details of ResNet18 on CIFAR100. The red star denotes the final  $K$ .

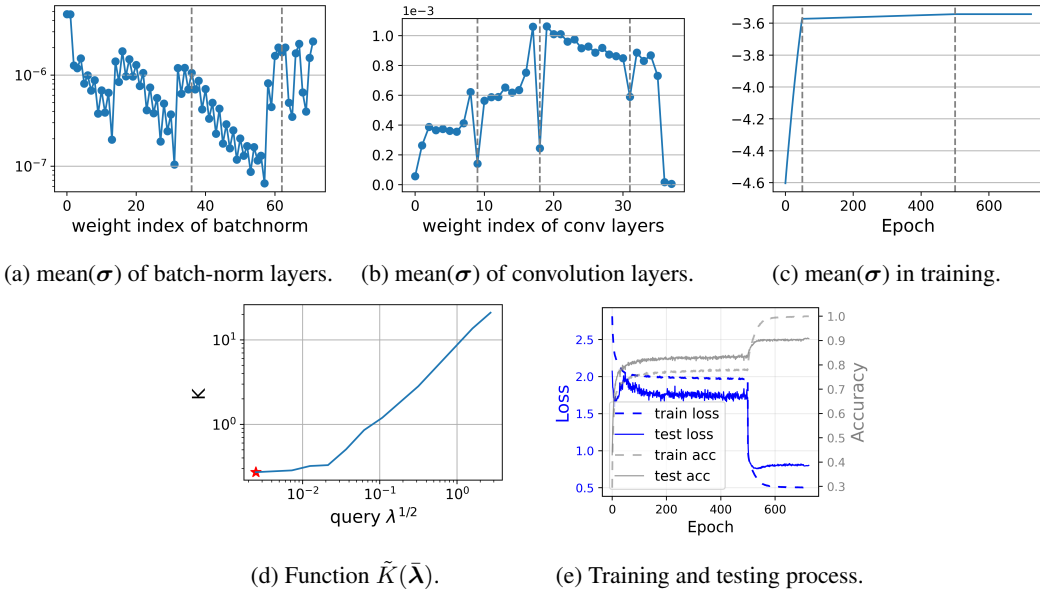


Figure 12: Training details of ResNet34 on CIFAR10. The red star denotes the final  $K$ .

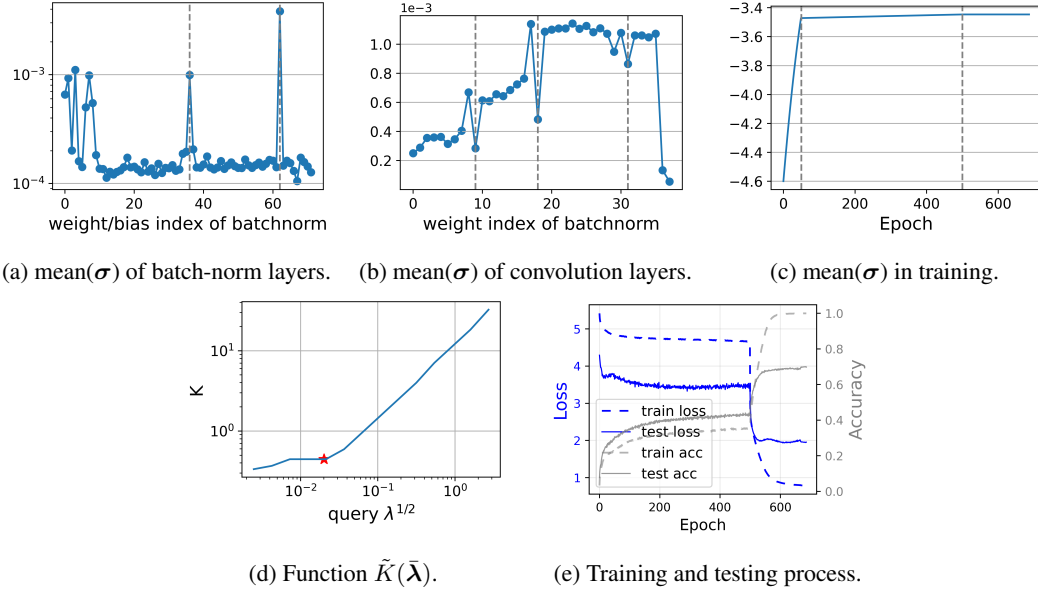


Figure 13: Training details of ResNet34 on CIFAR100. The red star denotes the final  $K$ .

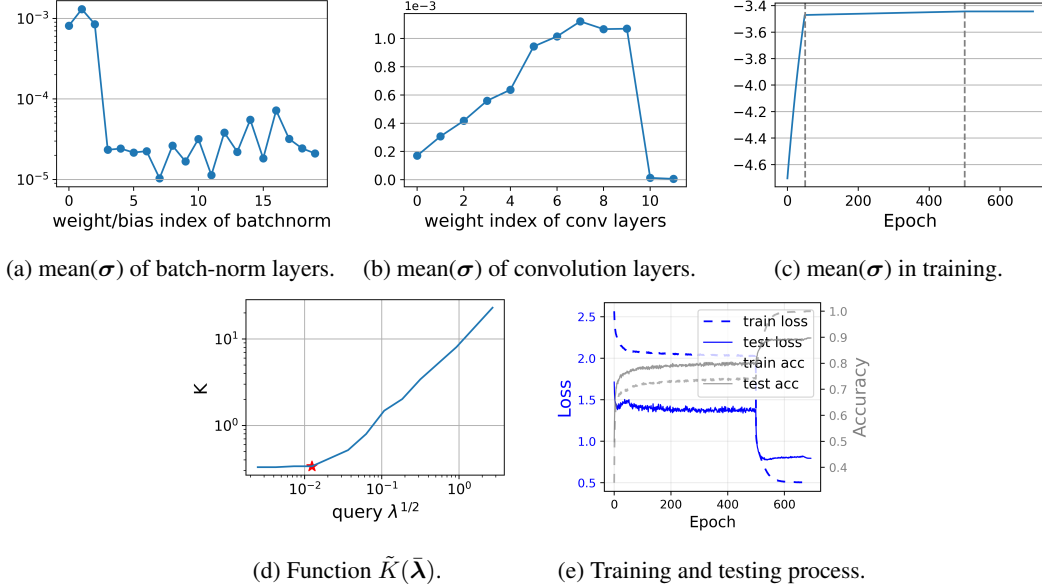
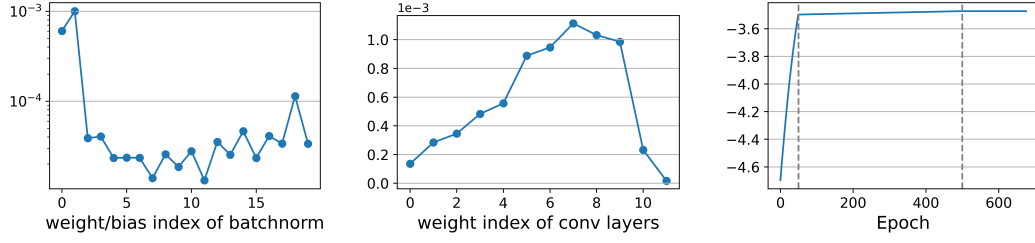
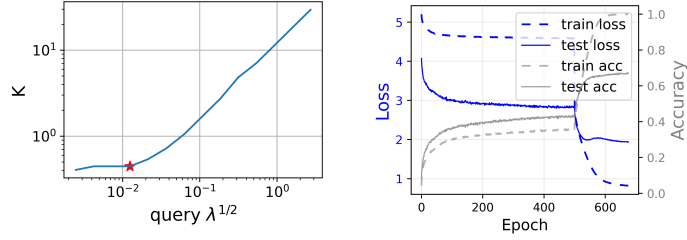


Figure 14: Training details of VGG13 on CIFAR10. The red star denotes the final  $K$ .



(a) mean( $\sigma$ ) of batch-norm layers. (b) mean( $\sigma$ ) of convolution layers. (c) mean( $\sigma$ ) in training.



(d) Function  $\tilde{K}(\bar{\lambda})$ . (e) Training and testing process.

Figure 15: Training details of VGG13 on CIFAR100. The red star denotes the final  $K$ .

## References

- [1] Pytorch-cifar. <https://github.com/kuangliu/pytorch-cifar/tree/master>. Accessed: 2020-05-24.
- [2] Pierre Alquier. User-friendly introduction to pac-bayes bounds. *arXiv preprint arXiv:2110.11216*, 2021.
- [3] Pierre Alquier and Benjamin Guedj. Simpler pac-bayesian bounds for hostile data. *Machine Learning*, 107(5):887–902, 2018.
- [4] Jean-Yves Audibert and Olivier Catoni. Robust linear least squares regression. 2011.
- [5] David GT Barrett and Benoit Dherin. Implicit gradient regularization. *arXiv preprint arXiv:2009.11162*, 2020.
- [6] Felix Biggs and Benjamin Guedj. Differentiable pac-bayes objectives with partially aggregated neural networks. *Entropy*, 23(10):1280, 2021.
- [7] Aleksandar Bojchevski and Stephan Günnemann. Deep gaussian embedding of graphs: Unsupervised inductive learning via ranking. *arXiv preprint arXiv:1707.03815*, 2017.
- [8] Stéphane Boucheron, Gábor Lugosi, and Pascal Massart. *Concentration Inequalities: A Nonasymptotic Theory of Independence*. Oxford University Press, 02 2013.
- [9] Olivier Catoni. A pac-bayesian approach to adaptive classification. *preprint*, 840, 2003.
- [10] Olivier Catoni. *Statistical learning theory and stochastic optimization: Ecole d’Eté de Probabilités de Saint-Flour, XXXI-2001*, volume 1851. Springer Science & Business Media, 2004.
- [11] Olivier Catoni. Pac-bayesian supervised classification: the thermodynamics of statistical learning. *arXiv preprint arXiv:0712.0248*, 2007.
- [12] Jeremy M Cohen, Simran Kaur, Yuanzhi Li, J Zico Kolter, and Ameet Talwalkar. Gradient descent on neural networks typically occurs at the edge of stability. *arXiv preprint arXiv:2103.00065*, 2021.
- [13] Alex Damian, Tengyu Ma, and Jason D Lee. Label noise sgd provably prefers flat global minimizers. *Advances in Neural Information Processing Systems*, 34:27449–27461, 2021.
- [14] Jacob Devlin, Ming-Wei Chang, Kenton Lee, and Kristina Toutanova. BERT: pre-training of deep bidirectional transformers for language understanding. *CoRR*, abs/1810.04805, 2018.
- [15] Gintare Karolina Dziugaite, Kyle Hsu, Waseem Gharbieh, Gabriel Arpino, and Daniel Roy. On the role of data in pac-bayes bounds. In *International Conference on Artificial Intelligence and Statistics*, pages 604–612. PMLR, 2021.
- [16] Gintare Karolina Dziugaite and Daniel M Roy. Computing nonvacuous generalization bounds for deep (stochastic) neural networks with many more parameters than training data. *arXiv preprint arXiv:1703.11008*, 2017.
- [17] Gintare Karolina Dziugaite and Daniel M. Roy. Computing nonvacuous generalization bounds for deep (stochastic) neural networks with many more parameters than training data. In *Proceedings of the 33rd Annual Conference on Uncertainty in Artificial Intelligence (UAI)*, 2017.
- [18] Gintare Karolina Dziugaite and Daniel M Roy. Data-dependent pac-bayes priors via differential privacy. *Advances in neural information processing systems*, 31, 2018.
- [19] Johannes Gasteiger, Aleksandar Bojchevski, and Stephan Günnemann. Predict then propagate: Graph neural networks meet personalized pagerank. *arXiv preprint arXiv:1810.05997*, 2018.
- [20] Jonas Geiping, Micah Goldblum, Phillip E Pope, Michael Moeller, and Tom Goldstein. Stochastic training is not necessary for generalization. *arXiv preprint arXiv:2109.14119*, 2021.
- [21] Pascal Germain, Alexandre Lacasse, François Laviolette, and Mario Marchand. Pac-bayesian learning of linear classifiers. In *Proceedings of the 26th Annual International Conference on Machine Learning*, pages 353–360, 2009.
- [22] Avrajit Ghosh, He Lyu, Xitong Zhang, and Rongrong Wang. Implicit regularization in heavy-ball momentum accelerated stochastic gradient descent. In *The Eleventh International Conference on Learning Representations*.

- [23] Maxime Haddouche, Benjamin Guedj, Omar Rivasplata, and John Shawe-Taylor. Pac-bayes unleashed: Generalisation bounds with unbounded losses. *Entropy*, 23(10):1330, 2021.
- [24] Will Hamilton, Zhitao Ying, and Jure Leskovec. Inductive representation learning on large graphs. *Advances in neural information processing systems*, 30, 2017.
- [25] Kaiming He, Xiangyu Zhang, Shaoqing Ren, and Jian Sun. Delving deep into rectifiers: Surpassing human-level performance on imagenet classification. In *Proceedings of the IEEE international conference on computer vision*, pages 1026–1034, 2015.
- [26] Matthew Holland. Pac-bayes under potentially heavy tails. *Advances in Neural Information Processing Systems*, 32, 2019.
- [27] Gao Huang, Zhuang Liu, Laurens Van Der Maaten, and Kilian Q Weinberger. Densely connected convolutional networks. In *Proceedings of the IEEE conference on computer vision and pattern recognition*, pages 4700–4708, 2017.
- [28] Thomas N Kipf and Max Welling. Semi-supervised classification with graph convolutional networks. *arXiv preprint arXiv:1609.02907*, 2016.
- [29] Alex Krizhevsky, Geoffrey Hinton, et al. Learning multiple layers of features from tiny images. 2009.
- [30] Ilja Kuzborskij and Csaba Szepesvári. Efron-stein pac-bayesian inequalities. *arXiv preprint arXiv:1909.01931*, 2019.
- [31] John Langford and Matthias Seeger. *Bounds for averaging classifiers*. School of Computer Science, Carnegie Mellon University, 2001.
- [32] Sungyoon Lee and Cheongjae Jang. A new characterization of the edge of stability based on a sharpness measure aware of batch gradient distribution. In *The Eleventh International Conference on Learning Representations*.
- [33] Gaël Letarte, Pascal Germain, Benjamin Guedj, and François Laviolette. Dichotomize and generalize: Pac-bayesian binary activated deep neural networks. *Advances in Neural Information Processing Systems*, 32, 2019.
- [34] Guy Lever, François Laviolette, and John Shawe-Taylor. Tighter pac-bayes bounds through distribution-dependent priors. *Theoretical Computer Science*, 473:4–28, 2013.
- [35] Aitor Lewkowycz, Yasaman Bahri, Ethan Dyer, Jascha Sohl-Dickstein, and Guy Gur-Ari. The large learning rate phase of deep learning: the catapult mechanism. *arXiv preprint arXiv:2003.02218*, 2020.
- [36] Xiang Li, Shuo Chen, Xiaolin Hu, and Jian Yang. Understanding the disharmony between dropout and batch normalization by variance shift. In *Proceedings of the IEEE/CVF conference on computer vision and pattern recognition*, pages 2682–2690, 2019.
- [37] Ping Luo, Xinjiang Wang, Wenqi Shao, and Zhanglin Peng. Towards understanding regularization in batch normalization. *arXiv preprint arXiv:1809.00846*, 2018.
- [38] Andreas Maurer. A note on the pac bayesian theorem. *arXiv preprint cs/0411099*, 2004.
- [39] David McAllester. Simplified pac-bayesian margin bounds. In *Learning Theory and Kernel Machines: 16th Annual Conference on Learning Theory and 7th Kernel Workshop, COLT/Kernel 2003, Washington, DC, USA, August 24-27, 2003. Proceedings*, pages 203–215. Springer, 2003.
- [40] David A McAllester. Some pac-bayesian theorems. In *Proceedings of the eleventh annual conference on Computational learning theory*, pages 230–234, 1998.
- [41] David A McAllester. Pac-bayesian model averaging. In *Proceedings of the twelfth annual conference on Computational learning theory*, pages 164–170, 1999.
- [42] Arvind Neelakantan, Luke Vilnis, Quoc V Le, Ilya Sutskever, Lukasz Kaiser, Karol Kurach, and James Martens. Adding gradient noise improves learning for very deep networks. *arXiv preprint arXiv:1511.06807*, 2015.
- [43] Antonio Orvieto, Hans Kersting, Frank Proske, Francis Bach, and Aurelien Lucchi. Anticorrelated noise injection for improved generalization. In *International Conference on Machine Learning*, pages 17094–17116. PMLR, 2022.

- [44] Maria Perez-Ortiz, Omar Rivasplata, Benjamin Guedj, Matthew Gleeson, Jingyu Zhang, John Shawe-Taylor, Mirosław Bober, and Josef Kittler. Learning pac-bayes priors for probabilistic neural networks. *arXiv preprint arXiv:2109.10304*, 2021.
- [45] María Pérez-Ortiz, Omar Rivasplata, John Shawe-Taylor, and Csaba Szepesvári. Tighter risk certificates for neural networks. *The Journal of Machine Learning Research*, 22(1):10326–10365, 2021.
- [46] Omar Rivasplata, Ilja Kuzborskij, Csaba Szepesvári, and John Shawe-Taylor. Pac-bayes analysis beyond the usual bounds. *Advances in Neural Information Processing Systems*, 33:16833–16845, 2020.
- [47] Omar Rivasplata, Vikram M Tankasali, and Csaba Szepesvári. Pac-bayes with backprop. *arXiv preprint arXiv:1908.07380*, 2019.
- [48] Matthias Seeger. Pac-bayesian generalisation error bounds for gaussian process classification. *Journal of machine learning research*, 3(Oct):233–269, 2002.
- [49] John Shawe-Taylor and Robert C Williamson. A pac analysis of a bayesian estimator. In *Proceedings of the tenth annual conference on Computational learning theory*, pages 2–9, 1997.
- [50] Karen Simonyan and Andrew Zisserman. Very deep convolutional networks for large-scale image recognition. *arXiv preprint arXiv:1409.1556*, 2014.
- [51] Christian Szegedy, Vincent Vanhoucke, Sergey Ioffe, Jon Shlens, and Zbigniew Wojna. Rethinking the inception architecture for computer vision. In *Proceedings of the IEEE conference on computer vision and pattern recognition*, pages 2818–2826, 2016.
- [52] Vladimir Vapnik and Vladimir Vapnik. Statistical learning theory wiley. *New York*, 1(624):2, 1998.
- [53] Petar Veličković, Guillem Cucurull, Arantxa Casanova, Adriana Romero, Pietro Lio, and Yoshua Bengio. Graph attention networks. *arXiv preprint arXiv:1710.10903*, 2017.
- [54] Colin Wei, Sham Kakade, and Tengyu Ma. The implicit and explicit regularization effects of dropout. In *International conference on machine learning*, pages 10181–10192. PMLR, 2020.
- [55] Wenda Zhou, Victor Veitch, Morgane Austern, Ryan P Adams, and Peter Orbanz. Non-vacuous generalization bounds at the imagenet scale: a pac-bayesian compression approach. *arXiv preprint arXiv:1804.05862*, 2018.